Susan Margaret Maciver

THE EFFECTS OF TRACE METAL CATIONS ON THE HIGH TEMPERATURE REACTIONS OF AN HALLOYSITE MINERAL

Submitted for the degree of
Master of Science in Chemistry
at the Victoria University of
Wellington, New Zealand.

1965.

ACKNOWLEDGEMENTS

CONTENTS

ABSTRACT

This thesis describes a kinetic study of the high
temperature solid state reactions of a well characterized
halloysite mineral and five of its cation-saturated forms, the
cations used being sodium, calcium, manganese, copper and iron
(III). The reaction sequence may be represented by the idealised
equations:

$$Al_2O_3.2SiO_2.4H_2O \xrightarrow{100^o - 300^oC} Al_2O_3.2SiO_2.2H_2O \qquad \ldots(a)$$

$$Al_2O_3.2SiO_2.2H_2O \xrightarrow{400^o - 600^oC} \underset{\text{metakaolinite}}{Al_2O_3.2SiO_2} + 2H_2O \qquad \ldots(b)$$

$$\underset{\text{metakaolinite}}{2(Al_2O_3.2SiO_2)} \xrightarrow{950^o - 1000^oC} \underset{\text{Al-Si Spinel}}{Si_3Al_4O_{12}} + SiO_2 \qquad \ldots(c)$$

$$\underset{\text{Al-Si Spinel}}{3(Si_3Al_4O_{12})} \xrightarrow{\sim 1100^oC} \underset{\text{mullite}}{2(3Al_2O_3.2SiO_2)} + \underset{\text{cristobalite}}{5SiO_2} \quad \ldots(d)$$
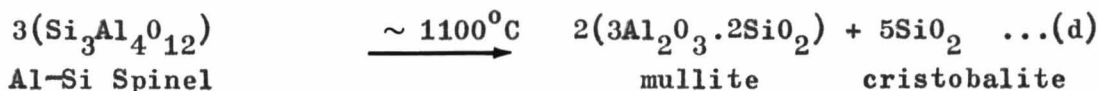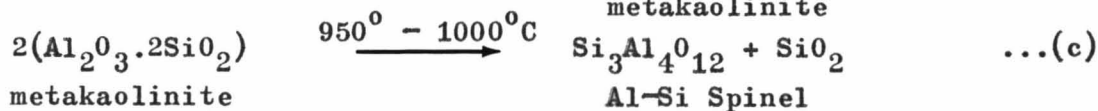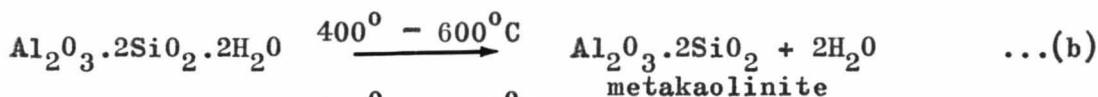
The formation of mullite from metakaolinite has been studied
in the temperature range $1020^o - 1200^oC$, by X-ray analysis.
Comparison of the experimental data with several theoretical
models suggests that up to 90% conversion the reaction takes
place by exponential nucleation followed by crystal growth.
There is, however, some evidence for diffusion occurring as a
rate controlling process, especially at high degrees of conversion
to mullite.

The rate constants and experimental thermodynamic functions have been evaluated for all halloysite samples. The free energies of activation $(111\text{--}128 \text{ k cal.mole}^{-1})$ and the rate constants are independent of the starting materials, but the enthalpies of activation $(51\text{--}118 \text{ k cal.mole}^{-1})$ and the entropies of activation $(0 \text{ to } -50 \text{ cal.deg.}^{-1}\text{mole}^{-1})$ are not.

INTRODUCTION

Clay minerals, being naturally occurring hydrated aluminosilicates, are used for various purposes in the ceramic industry. The nature and conditions of formation of the high temperature reaction products of the clays are functions of the physical and chemical properties of the minerals used. It is therefore of interest to investigate the effects of controlled variation of the chemical properties of the starting materials, to gain an insight into the influences of these variables on the processes taking place.

Halloysite is the hydrated form of kaolinite, and it occurs in two forms, $Al_2O_3 . 2SiO_2 . 2H_2O$ and $Al_2O_3 . 2SiO_2 . 4H_2O$. The latter dehydrates to the former at about $200-300^{\circ}C$, although the transformation temperature may be much lower, e.g. Grim (1) states that the irreversible dehydration may occur at temperatures as low as $60^{\circ}C$. The reaction sequence on heating may be represented by the idealized equations:

$$Al_2O_3.2SiO_2.4H_2O \xrightarrow{\ 100^{\circ} - 300^{\circ}C\ } Al_2O_3.2SiO_2.2H_2O$$

$$Al_2O_3.2SiO_2.2H_2O \xrightarrow{\ 400^{\circ} - 600^{\circ}C\ } \underset{\text{metakaolinite}}{Al_2O_3.2SiO_2} + 2H_2O$$

$$\underset{\text{metakaolinite}}{2(Al_2O_3.2SiO_2)} \xrightarrow{\ 950^{\circ} - 1000^{\circ}C\ } \underset{\text{Al-Si spinel}}{Si_3Al_4O_{12}} + SiO_2$$

$$3(Si_3Al_4O_{12}) \xrightarrow{\sim 1100^{\circ}C} 2(3Al_2O_3 \cdot 2SiO_2) + 5SiO_2$$

Al—Si spinel　　　　　　　　　　　　mullite　　cristobalite
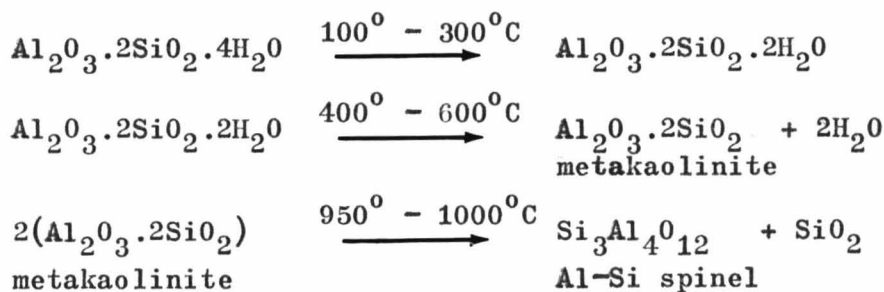
The clay mineral most often used by ceramic manufacturers is kaolinite. New Zealand, unlike most countries, has relatively large deposits of halloysite and small deposits of kaolinite. The widespread use of halloysite minerals in the New Zealand ceramic industry indicates the need for the type of study undertaken in the present work.

A differential thermal analysis (D.T.A.) trace of a typical halloysite has an endothermic peak corresponding to the initial dehydration, but, apart from this peak, the trace has the same general shape as that of a kaolinite. Between $400^{\circ}C$ and $600^{\circ}C$ there is a rapid loss of weight (2) due to the escape of hydroxyl water, the dehydrated product being known as meta-kaolinite. The D.T.A. trace has an endothermic peak in this region, and a large exothermic peak in the range $950^{\circ} - 1000^{\circ}C$. The most recent interpretation of this latter reaction is that of Brindley and Nakahira (3), who gave evidence for the formation of a cubic, close packed structure, an Al—Si spinel with vacant cation sites. When this spinel phase is heated to above $1100^{\circ}C$ the final phase, mullite, is formed, together with cristobalite, a high temperature form of silica, consisting of a three

dimensional diamond-type network of Si, with an O midway between each pair of the tetrahedrally disposed Si (4). Mullite is usually taken to be $3Al_2O_3.2SiO_2$, but it may vary to $2Al_2O_3.SiO_2$. The structure of mullite is believed to be orthorhombic, with defects (5), and with chains of Al-O octahedra running parallel to the c-axis, cross-linked by Al and Si in tetrahedral positions (6). Because of the variation in composition, there is a lack of precise definition of the structure of mullite.

MacKenzie (7) found that the addition of certain cationic impurities to an halloysitic mineral lowered the threshold temperature for mullite formation. On the basis of these results, the present work was begun. It is a study of the effects of the presence of trace metal cations on the kinetics and mechanism of the final stage in the series of reactions leading to the formation of mullite $3Al_2O_3.2SiO_2$, the clay mineral under investigation being an halloysite.

REFERENCES - INTRODUCTION

(1) GRIM, R.E.: "Applied Clay Mineralogy", p.14, McGraw-Hill, (1962).

(2) FREUND, F.: Ber.Dtsch.Keram.Ges. 37, 209 (1960).

(3) BRINDLEY, G.W. and NAKAHIRA, M.:   J.Am.Ceram.Soc. <u>42</u>, 311
     (1959).

(4) STILLWELL, C.:   "Crystal Chemistry", McGraw-Hill (1938).

(5) ĎUROVIČ, S.:   Ber.Dtsch.Keram.Ges. <u>40</u>, 287 (1963).

(6) TAYLOR, W.H.:   Z.Krist. <u>68</u>, 503-21 (1928).

(7) MACKENZIE, K.J.D.:   "The Kinetics and Mechanism of the
     High Temperature Solid State Reactions of Kaolinite
     Materials", M.Sc. Thesis, V.U.W. (1964).

CHAPTER 1

LITERATURE SURVEY

The general view (1) of the mechanism of mullite formation is not characterized by any great lucidity. This is largely because of the variation in local materials used in kinetic studies, and also because of the lack of precise information about the structure of mullite (2). For instance, several workers (3, 4) state that variations in the degree of crystallinity, and in the impurities associated with the original clay used may affect the character and proportion of the mullite phase.

According to Gehlen (5), the original plane of the kaolinite becomes the (111) plane of the spinel phase, and this becomes the (310) plane of mullite, the atomic arrangements remaining largely the same, especially those of oxygen. Brindley and Nakahira (2) propose a mechanism of mullite formation assuming that there is a continuity of the structure in the transitions upon heating, hence the oxygen framework remains while cations are removed. Mullite is believed (6)to be formed by the decomposition of the Al-Si spinel, which has vacant cation sites, thus providing a means for cation migration to take place.

1:1. The Structure of Halloysite

Halloysite is the hydrated form of the clay mineral, kaolinite, which belongs to the class of layer-type silicates. Kaolinite has a neutral double layer structure (7) and can be imagined to consist of a layer of SiO_4 tetrahedra in a two dimensional network connected via the apices of the tetrahedra with another two dimensional layer of $Al(OH)_6$ octahedra. Two-thirds of the OH groups of one side of the octahedral layer are imagined to be replaced by the O'' ions of the tetrahedra and the formula is thus $Al_2\left[(OH)_4/Si_2O_5\right]$. (See fig. 1A, 1B.) The neutral double layers of kaolin are believed to be held together by weak Van der Waal's forces, and kaolinite has a typical platy form.

The dihydrate form of halloysite has the same composition as kaolinite, but a different crystal form, and the water of hydration in $Al_2O_3.2SiO_2.4H_2O$ is believed to lie between kaolinite sheets in a monomolecular layer. X-ray diagrams of the dihydrate are consistent with a randomly displaced sequence of layers (9). The occurrence of a tubular form as revealed by electron micrographs has been attributed by Bates et al. (10) to curvature of the layers resulting from strain imposed by binding the Si-O and Al-OH layers together. Minimum strain

(i)
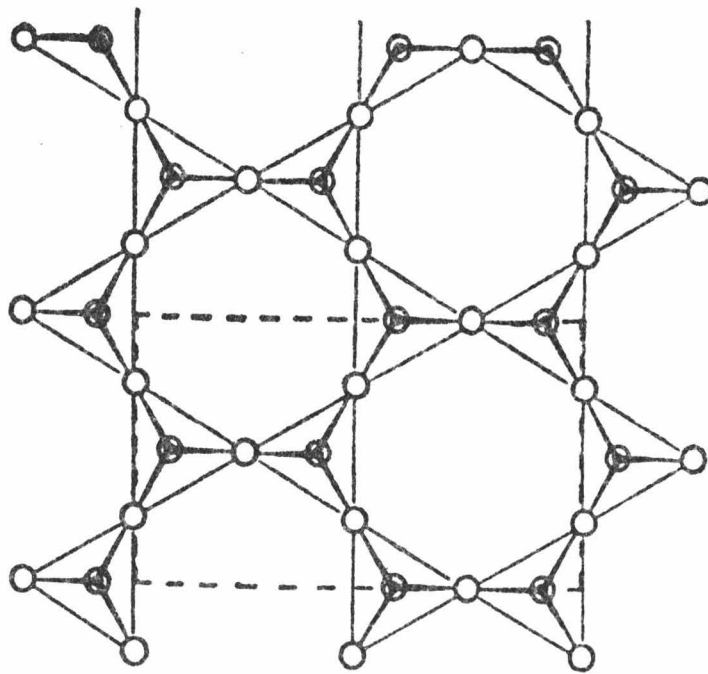
o Oxygen.

● Silicon.

(ii)
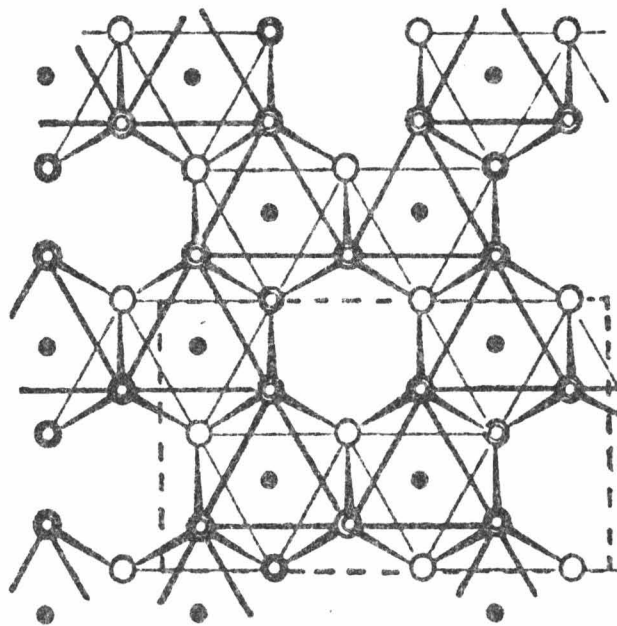
● Aluminium.
o Oxygen.
◉ Hydroxyl.

Fig.1 A.   Ideal configurations in Kaolin minerals.
(i) Tetrahedral, and (ii) Octahedral, Broken
lines show unit-cell boundary, after Brindley (7).
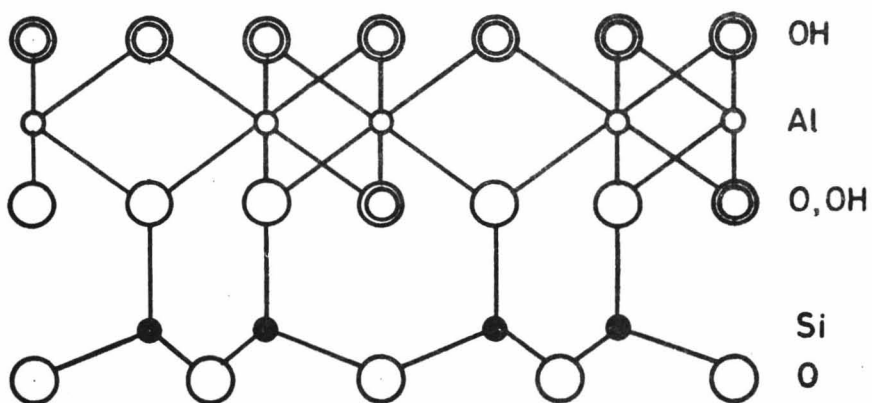
FIG. 1B STRUCTURE OF KAOLINITE.
PROJECTION ALONG A AXIS AFTER
BRINDLEY (8)

would be expected to exist in a layer which is curved so that the Si-O and Al-OH layers have, as nearly as possible, their own characteristic dimensions. Bates et al. (10) assume that in the hydrated halloysite a silicate sheet, of a certain radius characteristic of minimum strain, forms the innermost layer, and alternate layers of water and silicate may then be added externally with increasing radius, and therefore increasing strain, until the strain imposes a limitation on further growth. When dehydration occurs, the silicate layers either partially or completely collapse by removal of the interlayer water, producing broken fragments. Visconti (11) gave evidence that the tubular form persisted till $970^{o}C$ in some halloysites, but according to Grim (12), at high temperatures, an halloysite in general shows the properties of a kaolinite, particularly the poorly ordered form. (See fig. 1C.)

The existence of forms other than the typical tubular form has been demonstrated by several workers. Brindley (9), and Knapp and Mitra (13) observed, under an electron microscope, lath-like and fibrous forms, and according to Collins (14), it is sometimes observed in regular or spherical units. Sudo (15) found that halloysite sometimes showed rounded and irregular grains consisting of confused aggregates of very fine fibres, rather than hollow tubes.
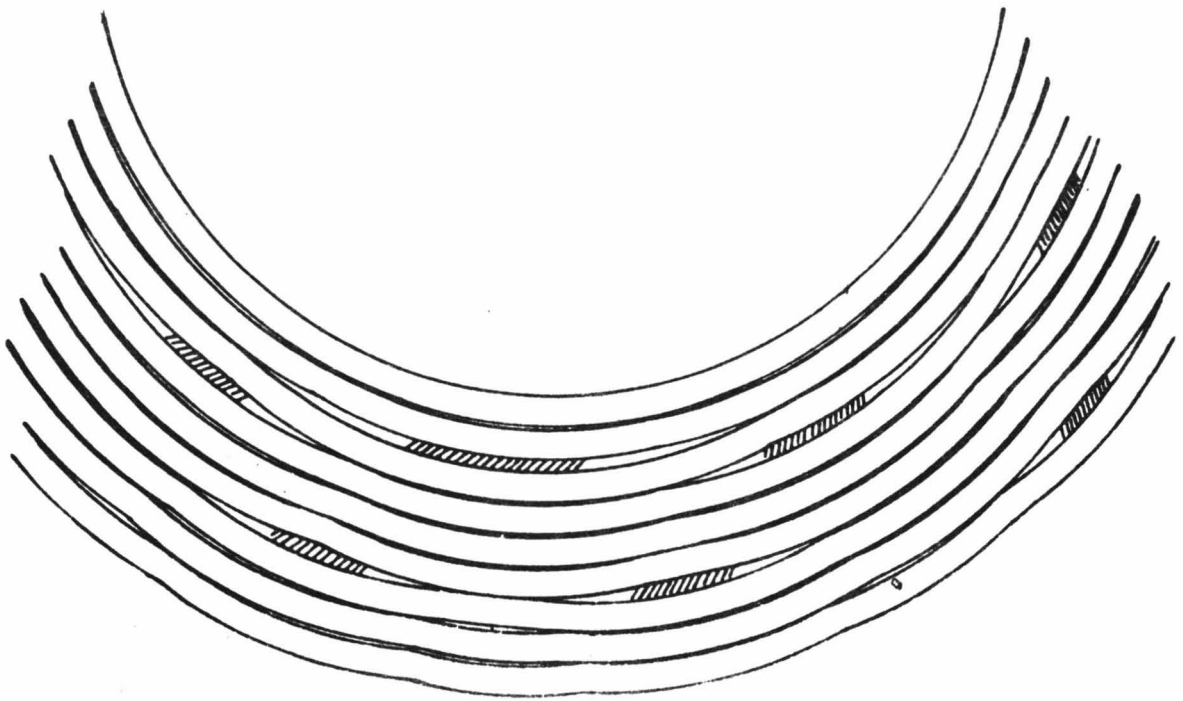
Fig.1c. Tubular structure of partially dehydrated halloysite with some residual water layers shown by shaded areas, after Brindley (9).

1:2. The Structures of Metakaolin, Al-Si Spinel, and Mullite

The mechanism proposed by Freund (6) for the formation of metakaolin and Al-Si spinel will serve to describe their structures. Freund assumes that between $400^{\circ}C$ and $600^{\circ}C$ OH groups are split off, two neighbouring OH groups combining with each other to form an H_2O molecule, which moves out of the crystal lattice by diffusion. One of the two O'' ions of the OH groups then forms a bridge between the two cations (Al^{3+} in this case) to which the OH groups were linked. It is possible that distortions of the tetrahedral lattice are increased by the splitting off of OH, but the coherence of the SiO_4 tetrahedral layer remains preserved (16). It is found (6) that there is a considerable discontinuous density increase, and also a discontinuous increase in electrical conductivity at about $950^{\circ}C$. On the basis of these two observations, metakaolin may be envisaged as a successive series of layers that are not densely packed, having large interspaces between individual layers. Support for this view has been given by Brindley and Nakahira (16), who found by X-ray studies that periodicity of kaolinite crystals had been destroyed along the c-axis, though the cohesion of the layers was not destroyed.

The large loss in energy during the reaction is understandable

if metakaolin represents a phase of high internal energy, due to empty interspaces between individual dehydrated layers. It is then imagined that when the framework collapses, this energy is released, and the spinel is formed. (See fig. 1D.) This spinel-type structure formed at about $950^\circ C$ is considered to be an Al-Si spinel with vacant cation sites (16). Mullite (see fig. 1E) is thought to be formed by the decomposition of the spinel, though the mechanism of this transformation is not well understood.

1:3. Previous Work on the Effects of Impurities on Mullite Formation

Sane and Cook (18) found that small additions of talc ($3MgO.4SiO_2.H_2O$) gave rise to increased mullite content in ceramic bodies, although increased amounts of talc, and higher temperatures, produced an increased proportion of a glassy phase. Parmelee and Rodriguez (19) found that the oxides of Mn, Zn, Li, Mg, Fe and Mo accelerated the formation of mullite, those of Na, K, Ti and Sn had a retarding effect, and those of B and Ca had no effect. Wahl (20) discovered that Mg, Fe, Pb, B and Ca in trace amounts enhanced, while alkali ions in general retarded mullite formation. He stated that additives had much the same effect on halloysite as on kaolinite, but were relatively more
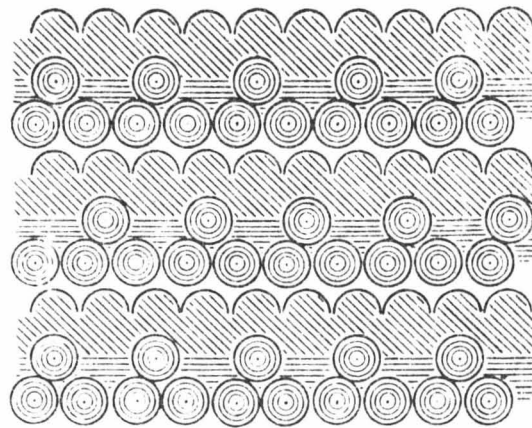
(a) Kaolinite.
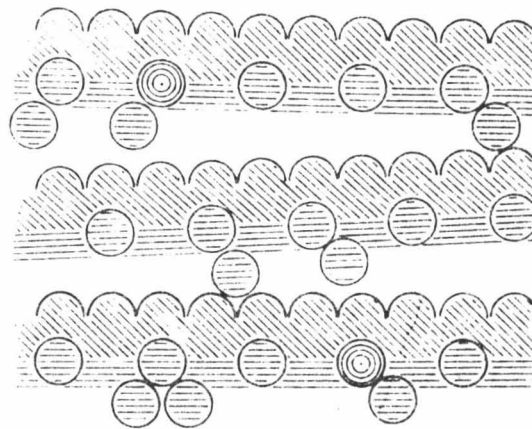
(b)Metakaolin.
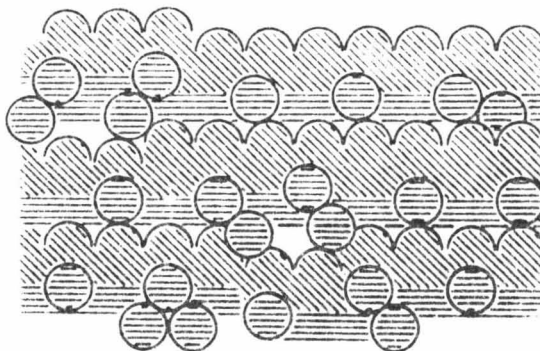
(c) Al-Si-spinel.

tetrahedral layer.
octahedral layer in which ⊚ is OH.
⊜ remaining O.

Fig.1D. Semi-schematic representation of the
thermal reactions of kaolinite ,after Freund (6)
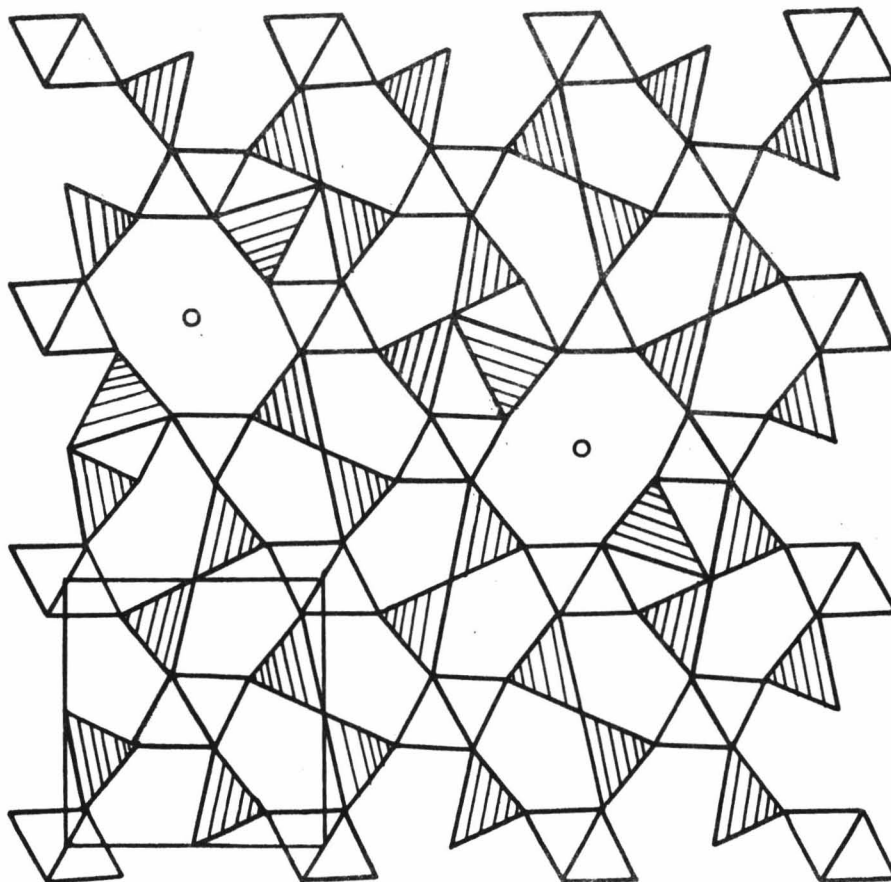
FIG. 1E REVISED MULLITE STRUCTURE,
IN POLYHEDRAL CO-ORDINATES, AFTER
DUROVIĆ (17)

effective in halloysite.   Kulbicki (21) found a large variation in the high temperature phases developed in montmorillonites with different exchangeable cations, and following treatment with salts of different concentrations.   MacKenzie (22) observed large variations in the rates of formation of mullite from an halloysite mineral treated with various cations.

If we assume that cation migration is a significant process in the mechanism of mullite formation, it is of interest to study the kinetic effects of variation in the impurity content of a particular clay mineral with a view to the elucidation of the mechanism of mullite formation, since it is apparent that the rate of mullite formation must bear some relation to the nature of the impurities present in the starting material.

1:4. Methods of Formation of Clays with Specific Exchanged Cations

All inorganic materials of small particle size have some exchange capacity due to broken bonds around the edges of the particles, this capacity increasing with decrease in particle size.   In theory, clays may be obtained in which all the exchangeable cations are replaced by a single cationic species. A number of methods are available for replacement of exchangeable cations with hydrogen ions.   Subsequently by base exchange with

selected cation sites it is in principle possible to prepare a clay in which all the exchange sites are occupied by the same cationic species.

The production of hydrogen saturated aluminosilicates (represented by HX) is not as simple as is implied by the equation:

$$H^+ + MX \longrightarrow HX + M^+$$

where M^+ is a metal ion (23). Hydrogen clays tend to become partly saturated with Al^{3+} and other ions, because ionic constituents within the lattice, in particular Al^{3+}, Fe^{3+}, Mg^{2+} and K^+ become mobile as the hydrogen ion content of the clay is developed.

Three general procedures are available for the preparation of the hydrogen clay:

(a) leaching with a salt solution, followed by dilute acid washing,

(b) electrodialysis,

(c) reaction of the clay with an acid organic exchange resin.

According to Grim (24) it is impossible to prepare clays in which all the exchange positions are occupied by H^+, since Al^{3+}

ions move in from the lattice to exchange positions before saturation with H^+ becomes complete. Kaolinite minerals, however, are affected least in this respect. This suggests that the more rapidly the process:

clay $\longrightarrow$ hydrogen clay $\longrightarrow$ specific cation clay

may be carried out, the more nearly will the situation be approached where all the exchange sites are occupied by the same cation.

The results of several workers (25) suggest that electro-dialysis, as a means of producing hydrogen clay, must be used with caution. Ovcharenko and Martsin (25) found that electro-dialysis of montmorillonite effected transfer of Al^{3+} from lattice to ion exchange positions, and gave rise to changes in dimensions between basal planes. Searle and Grimshaw (25) claim that in some clay minerals, the release of cations which are normally part of the structure, may cause a breakdown of the lattice by this method.

Of the three methods available, the use of an acid organic exchange resin appears to be the most satisfactory, for the following reasons:

(i)   It is considerably faster than (a) or (b).

(ii) It is more efficient than (a) or (b) (25c).

(iii) The mineralogical composition of the clays is much less likely to be affected by this method than by either of (a) or (b).

Since any mechanistic treatment of the high temperature reactions of a clay mineral with a specific exchanged cation would normally assume that the cation clay had the same basic structure, apart from the occupation of exchange positions, as the original clay, (iii) is of overriding importance.

1:5. Cation Exchange in Halloysites

The important chemical characteristic of all clays is that of cation exchange, as a result of the large surface area per unit of weight. The three causes (26) of cation exchange capacity in clays are believed to be:

(a) Broken bonds around the edges of silica-alumina units giving rise to unsatisfied charges which may be balanced by adsorbed cations.

(b) The H of exposed OH groups may be replaced by a cation which would be exchangeable.

(c) Substitutions within the lattice of Al^{3+} for Si^{4+} in the tetrahedral sheet, and also of ions of lower

valence for Al^{3+} (e.g. Mg^{2+}) in the octahedral sheet.

In the class of kaolinite minerals, the sites of exchange reactivity are generally agreed (27) to be associated with the hydroxyl groups on the exposed clay surfaces, this model being consistent with the low exchange capacities of such clays. In general the rate of cation exchange is almost instantaneous with kaolinite minerals (26). There are almost no replacements within the lattice in halloysites and kaolinites, because of the essentially neutral structures of these double layer silicates.

REFERENCES − CHAPTER 1

(1) LUNDIN, S.T.: "Studies on Triaxial Whiteware Bodies", p.8, Almquist and Wiksell, Stockholm, (1959).

(2) BRINDLEY, G.W. and NAKAHIRA, M.: J.Am.Ceram.Soc. 42, 314, (1959).

(3) LUNDIN, S.T.: "Studies on Triaxial Whiteware Bodies", p.38, Almquist and Wiksell, Stockholm, (1959).

(4) GLASS, H.D.: Am.Mineral. 39, 193 (1954).

(5) GEHLEN, K.V.: Ber.Dtsch.Keram.Ges. 39, 315−20 (1962).

(6) FREUND, F.: Ber.Dtsch.Keram.Ges. 37, 209 (1960).

(7) BRINDLEY, G.W. in "X−ray Identification and Structures of the Clay Minerals" Ed.G.Brown, p.54 (1961) Mineral.Soc.London.

(8) BRINDLEY, G.W. in "X-ray Identification and Structures of the Clay Minerals" Ed.G.Brown, p.55-62 (1961) Mineral. Soc. London.

(9) BRINDLEY, G.W. in "Clays and Clay Technology" (Ed. J.A. Pask and M.D. Turner) 1st National Conference on Clays and Clay Technology, San Francisco (1955).

(10) BATES, T.F.; HILDEBRAND, F.A.; and SWINEFORD, A.: Am. Mineral. 35, 463-484 (1950).

(11) VISCONTI, Y.S.: Second Conference on Ceramics, Brazil (1956).

(12) GRIM, R.E.: "Applied Clay Mineralogy", p.16-18, McGraw-Hill (1962).

(13) KNAPP, D.R. and MITRA, R.P.: Nature, London 166, p.380-1, (1951).

(14) COLLINS, B.J.S.: "Textural Morphological Studies of Some Clay Minerals", Ph.D. Thesis, University of Illinois (1955).

(15) SUDO, Toshio: Mineral.Journ.(Japan) 1, 66-68, (1953).

(16) BRINDLEY, G.W. and NAKAHIRA, M.: J.Am.Ceram.Soc. 42, 311 (1959).

(17) ĎUROVIČ, S.: Ber.Dtsch.Keram.Ges. 40, 287 (1963).

(18) SANE, S. and COOK, R.L.: J.Am.Ceram.Soc. 34, 145 (1951).

(19) PARMELEE, C.W. and RODRIGUEZ, A.R.: J.Am.Ceram.Soc. 25, 1-10 (1942).

(20) WAHL, F.M.: "Reactions in Kaolin-Type Minerals at Elevated
      Temperatures as Investigated by Continuous X-ray
      Diffraction", Ph.D. Thesis, University of Illinois (1958).

(21) KULBICKI, G. in "Clays and Clay Minerals", p.144-158, 5th
      National Conference on Clays and Clay Minerals,
      Washington (1958).

(22) MACKENZIE, K.J.D.: "The Kinetics and Mechanism of the High
      Temperature Solid State Reactions of Kaolinite Minerals",
      M.Sc. Thesis, V.U.W. (1964).

(23) JACKSON, M.L.: "Soil Chemical Analysis: Advanced Course",
      Ch.16, M.L. Jackson, Wisconsin.

(24) GRIM, R.E.: "Clay Mineralogy", p.142, McGraw-Hill (1953).

(25)(a) OVCHARENKO, F.D. and MARTSIN, T.: Dopovidi Akad. Nauk.
      Ukr. R.S.R. 649-54 (1960).

   (b) SEARLE, A.B. and GRIMSHAW, R.W.: "The Chemistry and
      Physics of Clays", 3rd Ed., p.264, Benn (1959).

   (c) LEWIS, D.R. in "Clays and Clay Technology" (Ed. J.A. Pask
      and M.D. Turner), p.63, 1st National Conference Clays
      and Clay Technology, San Francisco (1955).

   (d) GRIM, R.E.: "Clay Mineralogy", p.300, McGraw-Hill (1953).

(26) GRIM, R.E.: "Applied Clay Mineralogy", p.15, McGraw-Hill
      (1962).

(27)(a) BUEHRER, T.F. in "Clays and Clay Technology" (Ed. J.A. Pask and M.D. Turner), 1st National Conference Clays and Clay Technology, San Francisco (1955).

(b) MIELENZ, R.C. and KING, M.E.: Ibid, p.209.

(c) LEWIS, D.R.: Ibid, p.54.

(d) ALEXANDER, A.E. and JOHNSON, P.: "Colloid Science", Vol.II, Oxford (1949).

(e) SEARLE, A.B. and GRIMSHAW, R.W.: "The Chemistry and Physics of Clays", Benn 3rd Ed., p.267 (1959).

CHAPTER 2

EXPERIMENTAL METHODS

If any valid interpretation of the experimental results of kinetic studies of mullite formation in a clay mineral is to be made, the starting material should be of known composition and type. The mineral used in this kinetic study was subjected to physical and chemical investigation.

MacKenzie (1) has made a literature survey of the previous methods of study of mullite formation, and on the basis of his findings a method of analysis of mullite by X-ray was used throughout this work. The method was devised by MacKenzie, and is a quantitative X-ray powder diffraction analysis using an internal standard.

2-1. Properties of the Halloysite

The sample used in the present kinetic study was an halloysite mineral, from a deposit on Sharp's farm seven miles west of Te Puke, New Zealand. The D.T.A. trace (Fig. 2A) is of a typical halloysite, and the X-ray trace (Fig. 2B) indicates that the major mineral is halloysite, which accounts for all the reflections.

Chemical analyses of the mineral gave the following results:

Size fraction – 0·5 – 2μ E.S.D.

Heating rate – 10°/ min
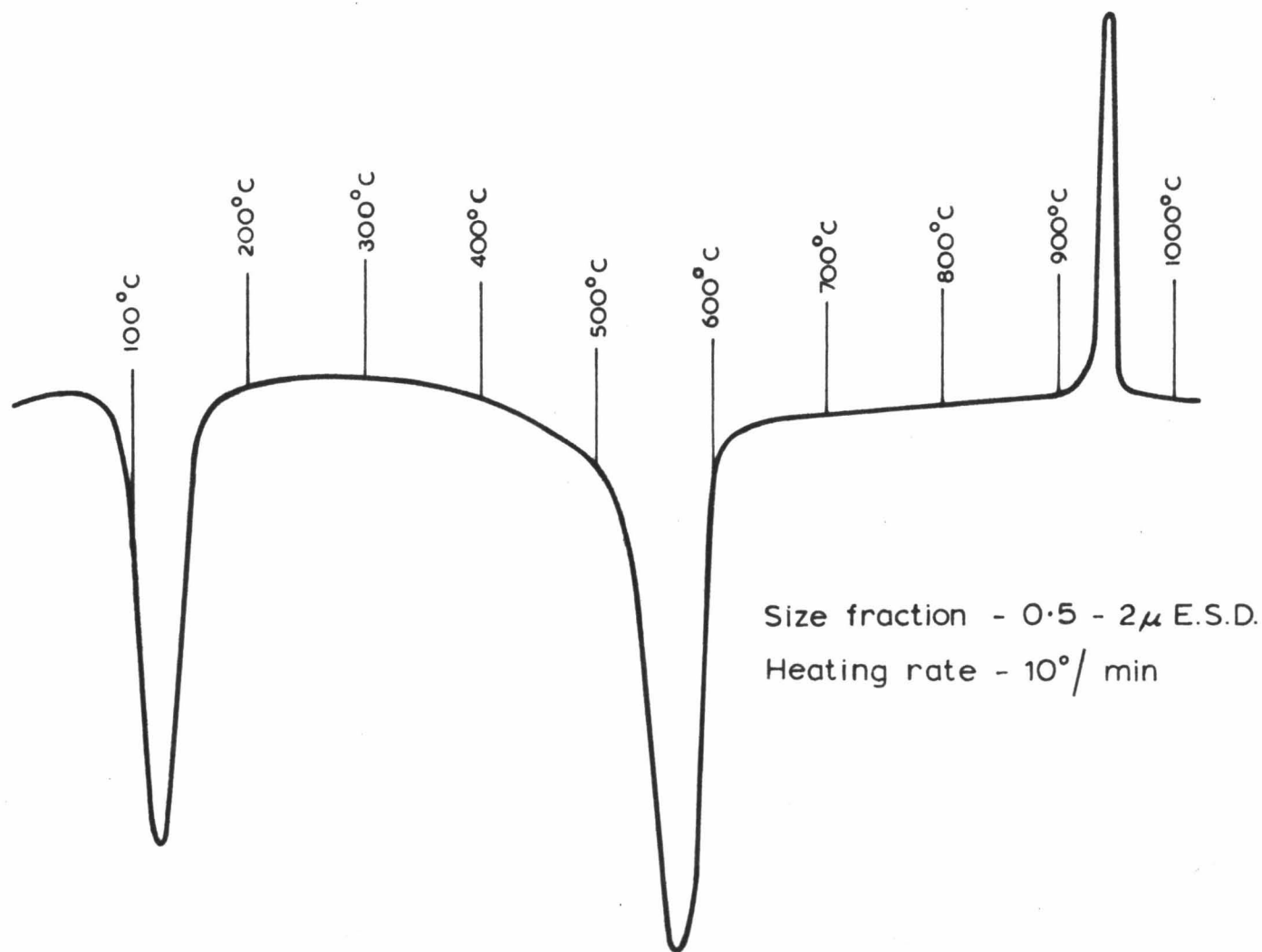
FIG. 2A DIFFERENTIAL THERMAL ANALYSIS PATTERN

OF HALLOYSITE SAMPLE

Size fraction - 0·5 - 2μ E.S.D.
Radiation - Cu Kα
Filter - Ni
Scan speed - 1° 2θ/min
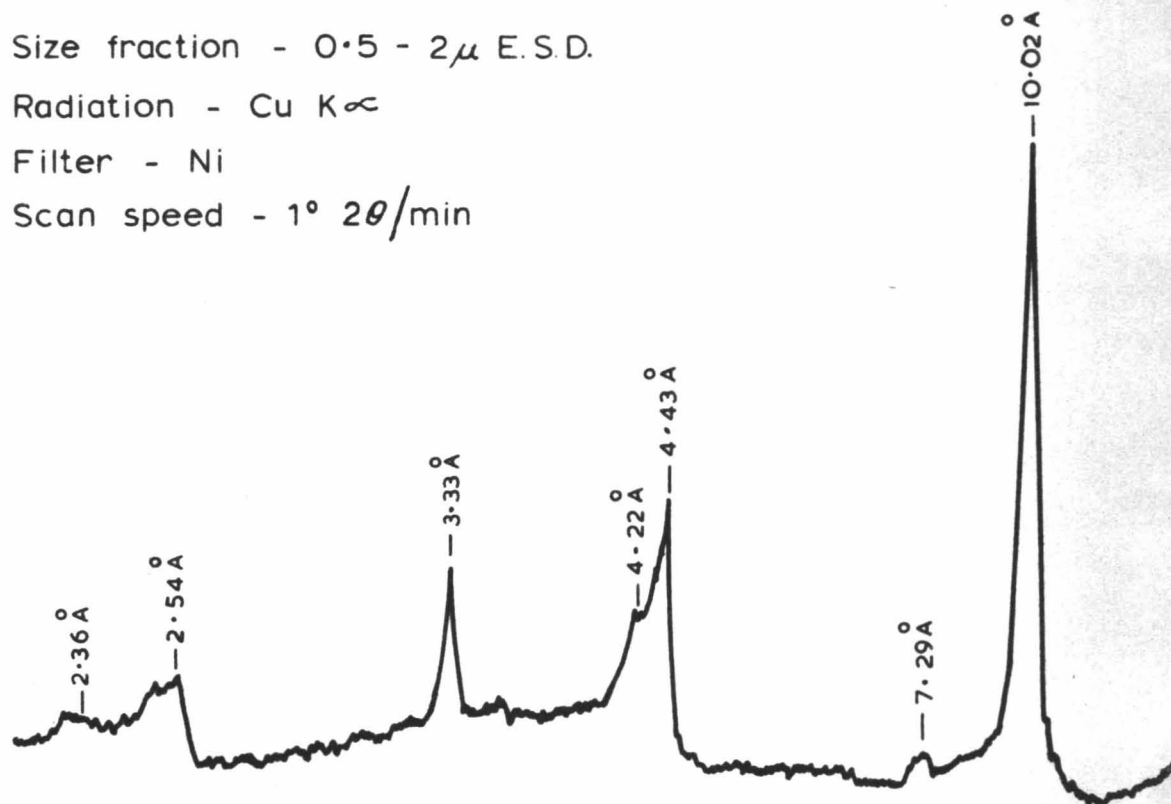
FIG. 2B X-RAY DIFFRACTION PATTERN OF RELATIVELY UNORIENTED POWDER SAMPLE OF HALLOYSITE

Table 1. Chemical Analyses of the Halloysite

Compound	% by weight
SiO_2	41.03
TiO_2	0.1
Al_2O_3	32.92
Fe_2O_3	3.6
CaO	0.04
MgO	0.06
Na_2O	0.1
K_2O	<0.1
$H_2O(+)$	8.95
$H_2O(-)$	13.1

If the halloysite is imagined to have the idealised chemical formula, there is about 1% of SiO_2 which is not accounted for.

Semi-quantitative emission spectrographic analyses of trace elements were performed, using a D.C. arc method. The results are given in Table 2, correct to $\pm$ 50% of the content.

Table 2. D.C. Arc Analyses of the Halloysite

Element	% by weight
Co	<0.01
Mn	0.002
Mg	0.03
Ni	<0.01

2-2. The X-ray Analytical Method

The essential features of the powder diffraction technique include a narrow beam of monochromatic X-rays impinging on a crystalline powder composed of fine, randomly oriented particles. In a powder sample every possible crystal face and plane is exposed to the incident X-ray beam, so that all diffractions will be observed.

The Bragg equation (2, 1) gives the conditions for a diffracted beam (2).

$$n \lambda \quad = \quad 2d \sin \Theta \qquad\qquad \dots\dots\dots (2, 1)$$

where   n is an integer, known as the "order" of the reflection

λ is the wavelength of the X-rays

d is the inter-planar spacing between successive planes in the crystal

Θ is the angle between the atomic plane and both of the incident and "reflected" beams.

When the sample is rotated through all possible incident angles in the X-ray beam, every allowable diffraction will be observed.   The scattered X-rays may be detected by a camera, or by a rotating Geiger counter connected to a recorder or ratemeter system.   Throughout the present work a Geiger counter connected

to a recorder system was used for detection.

A powder diffraction pattern is characteristic of a given substance, and each substance in a mixture produces its pattern independently of the others (3). If we assume that, apart from absorption of X-rays by the sample, the intensities of the peaks of each component are proportional to the amount of component present in the sample, then a quantitative analysis of the various components may be developed.

Any absolute quantitative determination of mullite in powder samples, made on the assumption that the area of a peak characteristic of a substance is proportional to the concentration of the substance, usually depends also on the following assumptions:

(a) The X-ray source is of constant output.

(b) The counting procedures are reproducible.

(c) The mass absorption coefficient of the sample for X-rays has negligible influence.

Clark and Reynolds (4) developed a method of quantitative analysis based on the use of an internal standard to correct for the errors arising from the above assumptions. This technique involves the intimate mixing of a fixed percentage by weight of

some reference material with the sample. The ratio of sample peak area to reference peak area is then measured. The method introduces a new assumption, viz. that the X-ray intensity does not change over the interval between the sample and reference peaks.

2-3. Preparation of the Calibration Curve

A calibration curve was needed for the analysis of mullite. The preparation of standard mullite was complicated by the wide variation in the stoichiometric composition of mullite formed under different conditions. It was therefore necessary to prepare the standard mullite under conditions similar to those of the reaction, by firing a sample of the mineral, molochite, to $1490^{o}C$, and treating it with hydrofluoric acid to remove any glass. The sample obtained gave an X-ray trace having the reported peak positions and intensities of mullite (5).

The standard mullite was diluted with feldspar glass, prepared by firing feldspar to $1500^{o}C$ and grinding to < 100 mesh. The diluted samples were then ground in a mechanical mortar for 0.5 hours and mixed with 5% barium fluoride (by weight) as the internal standard. The grinding time was chosen as 0.5 hours for all samples, since the intensity ratio of sample peak area (mullite) to reference peak area (BaF_2) reached a maximum as the

particle size decreased, attaining a limiting value after about 0.5 hours grinding (1).

The calibration curve (Fig. 2c) was determined using the ratio of the mullite doublet peak at d = 3.41$\overset{o}{A}$ to the BaF_2 reference peak at d = 3.58$\overset{o}{A}$.

2-4. Errors in the Quantitative Analysis

The major sources of error in the quantitative analysis, apart from those arising because of mechanical grinding inconsistencies, were:

(a) preferential orientation of the sample particles,

(b) incomplete mixing of the reference material with the sample,

(c) insufficient scans to give good counting statistics,

(d) measurement of peak areas,

(e) assumption that X-ray analysis will reveal all of the mullite present in a sample.

Relatively unoriented samples were prepared by a method devised by MacKenzie (1). The samples were packed at random from the back into a rectangular slot in an aluminium plate lying on a sheet of glass. The back was smoothed off and sealed with a glass cover slip and adhesive tape; the whole system was then
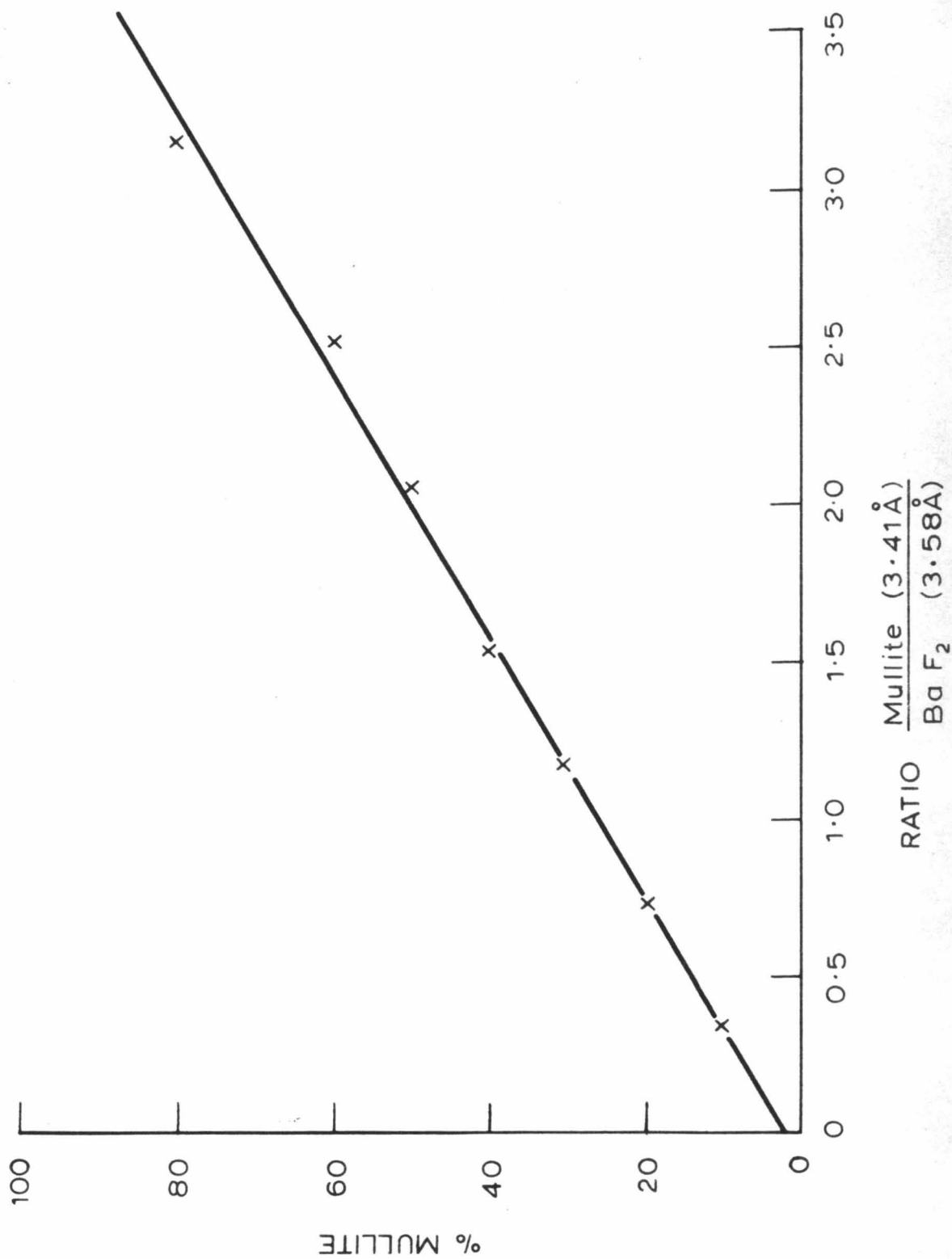
FIG. 2C MULLITE CALIBRATION CURVE

inverted and the glass plate removed. By this means preferential
orientation was reduced as far as was practicable.

A standard procedure of light hand mixing for about three
minutes was used to minimise the error arising from incomplete
mixing of the BaF_2 and the sample.

Five scans of the same peak were chosen for all analyses, as
a compromise between analysis time and reproducibility.

The largest source of error was that of peak area measurement,
especially at low mullite concentrations. The error was minimised
by adopting a procedure of cutting out and weighing peaks, the
resultant error being to a large extent reduced by the amount of
care taken. Error was introduced in the judgement of the base
line through the background. Reproducibility was found to be
worse for fired samples, particularly with low firing times, when
the line profiles of the mullite peaks were diffuse and certainly
not of doublet form. The only significant property of a reflection
for the derivation of unit cell dimensions is its position, but
for information about the crystal texture, the distribution of
intensity as a function of angle is the property required. In
the region where the peaks are diffuse, it is difficult to say
whether the poorly crystalline substance producing the peaks
really is mullite.

The error arising from the last source mentioned above is not measurable, but it almost certainly exists.   X-ray analyses of mullite at low firing temperatures and/or low firing times may not reveal enough of the new mullite because the new units may be too small or imperfect to cause diffraction (6).

For fired samples, a reproducibility of $\pm$ 5% was obtained, with practice.

2-5.   Preparation of Materials for Firing

The size fraction of clay used throughout the kinetic work was 0.5 - 2μ Equivalent Spherical Diameter (E.S.D.).   The particles of > 2μ E.S.D. were removed by dispersing the sample in water with 2% sodium hexametaphosphate, and suitably adjusting the settling time.   The 0.0 - 2μ E.S.D. size fraction was obtained from the suspension by passage through a filter press.   The dispersing agent was washed out, the sample redispersed in distilled water, and the required fraction was centrifuged out for 9.0 minutes at 1500 r.p.m., the figures being calculated from Stokes' (1) Law for an equivalent spherical body.

Extruded rods were used for firing throughout the present work.   They were obtained by preparation of a thick paste of the sample with distilled water, followed by passage through a small

41.

1/8 in. manual extruder. The rods were oven dried at $110^{o}C$, and prefired up to $650^{o}C$, to ensure that the dehydroxylation reaction was as complete and as uniform as possible.

Firing was carried out in crucibles made of refractory bricks designed to have minimum heat capacity. They were prefired up to $1100^{o}C$ to complete any unwanted reactions, and to remove moisture. A powder layer of the sample was laid down in the bottom of each crucible to reduce diffusion of the reaction products from the firebrick into the sample, or vice versa. Samples of about 0.5 grams were placed in the crucibles and inserted all together in the furnace at a preselected temperature. The temperature was kept approximately constant by manual control, the error being less than $\pm$ $10^{o}C$ over the greater part of any run.

After the required firing times the samples were removed, air quenched, and ground for 0.5 hours in a mechanical mortar. 5% by weight of BaF_2 was then added, and X-ray analyses for mullite were performed.

REFERENCES - CHAPTER 2

REFERENCES - CHAPTER 2

(1) MACKENZIE, K.J.D.: "The Kinetics and Mechanism of the High Temperature Solid State Reactions of Kaolinite Minerals", M.Sc. Thesis, V.U.W. (1964).

(2) BRAGG, W.L.: Proc. Cambridge Phil. Soc. 17, 43 (1912).

(3) KLUGG, H.P. and ALEXANDER, L.E.: "X-Ray Diffraction Procedures",
     p.410 Wiley (1954).

(4) CLARK, G.L. and REYNOLDS, D.H.: Ind.Eng.Chem.; Anal.Ed. $\underline{8}$,
     36 (1936).

(5) BROWN Ed.: "X-Ray Identification and Structure of the Clay
     Minerals", p.485. Mineral.Soc.London (1961).

(6) GRIM, R.E.: "Applied Clay Mineralogy", p.96 McGraw-Hill (1962).

CHAPTER 3

EXPERIMENTAL RESULTS FOR UNTREATED HALLOYSITE

The untreated halloysite is, in effect, a control sample, relative to which the kinetics and mechanism of mullite formation in cationic clays are observed.

3-1. Growth Curves for Mullite

Fig. 3A gives the growth curves of mullite for the untreated halloysite at temperatures of $1080^{o}C$, $1110^{o}C$, $1140^{o}C$, $1170^{o}C$ and $1200^{o}C$. The rate was too fast to measure by the X-ray method at temperatures above $1200^{o}C$, and mullite was not formed in measurable amounts below $1080^{o}C$.

The growth curves were scaled to the same axes by plotting $\frac{C}{C_\infty}$ versus $\frac{t}{t_{0.85}}$, where C = % mullite at time t

$$C_\infty = \text{\% mullite at time } t = \infty$$

$$t_{0.85} = \text{time required for 85\% conversion}$$

$$\text{of mullite.}$$

When all the growth curves were scaled to the same axes, the resultant curves were superimposable (Fig. 3B), which suggests that the same mechanism for mullite formation may occur at all temperatures.
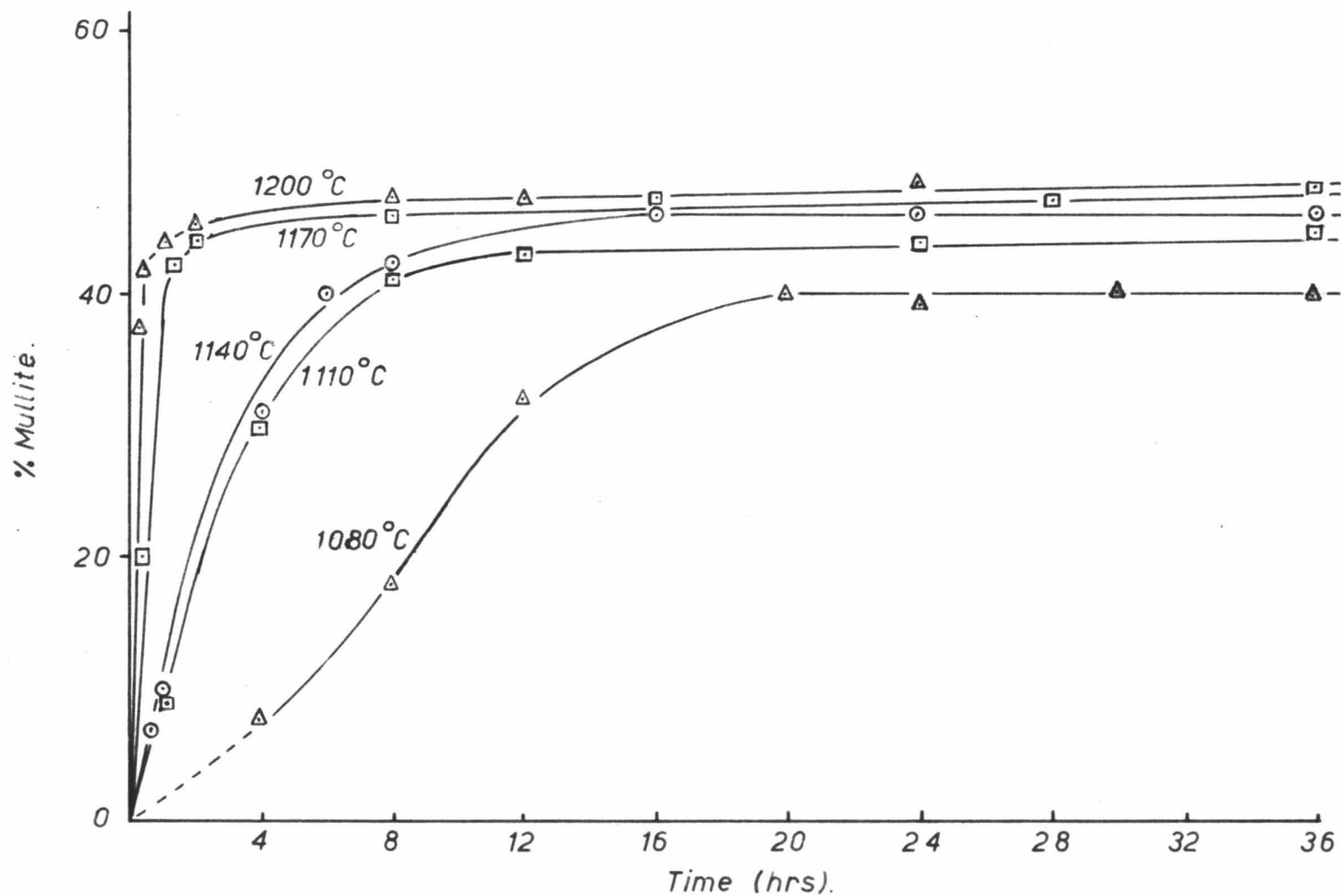
Fig.3 A. Mullite growth curves from untreated Halloysite.
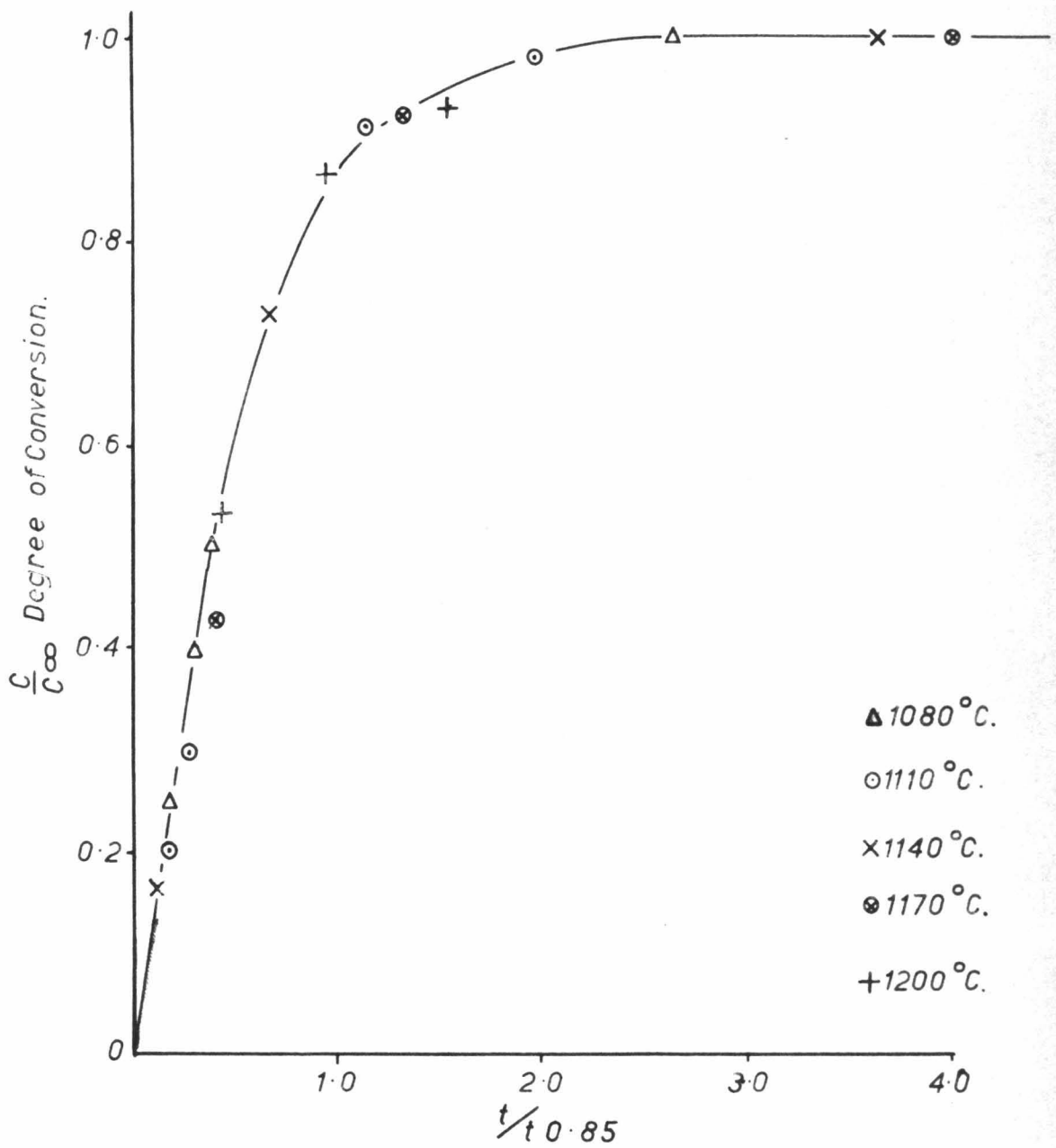
Fig. 3 B.   Reduced growth curve.

3-2. Evaluation of the Thermodynamic Functions

The values for the absolute reaction rates R were obtained from the slopes of tangents to the growth curves at various values of α, where $\alpha = \dfrac{C}{C_\infty}$. Rate constants for the reaction were found from the intercepts of graphs of log R versus log α on the log R axis. The rate constants are given in Table 1.

From absolute rate theory (1), the following expression is derived for the rate constant:

$$K = \frac{RT}{Nh} \exp\left\{\frac{\Delta S^*}{R}\right\} \ \exp\left\{\frac{-\Delta H^*}{RT}\right\} \qquad \ldots\ldots(3, 1)$$

$$= \frac{RT}{Nh} \exp\left\{\frac{-\Delta G^*}{RT}\right\} \qquad \ldots\ldots(3, 2)$$

Equation (3, 2) gives:

$$\Delta G^* = RT\left[\ln\left(\frac{RT}{Nh}\right) - \ln K\right] \qquad \ldots\ldots(3, 3)$$

Substitution for K in (3, 3) leads to the value of ΔG^*. The ΔG^* values obtained are shown in Table 2.

ΔH^* values were obtained from the slopes of lines of log $t_{\frac{1}{2}}$ versus $1/T$. The values for ΔH^* are given in Table 2.

ΔS^* was found from the definition:

$$\Delta S^* = \frac{\Delta H^* - \Delta G^*}{T} \qquad \ldots\ldots(3, 4)$$

The function $(3, 4)$ is subject to a very large percentage error, since it involves the difference of two quantities which have very nearly the same values. The Δ S* are given in Table 2.

Table 1. Rate Constants

Temp. (^{o}C)	1080	1110	1140	1170	1200
K(sec.$^{-1}$)	1.97×10^{-6}	1.97×10^{-6}	2.54×10^{-6}	5.55×10^{-6}	3.84×10^{-6}

Table 2. Thermodynamic Functions

Temp. (^{o}C)	1080	1110	1140	1170	1200
Δ H*(K cal.mole^{-1})	118	118	118	118	118
Δ G*(K cal.mole^{-1})	118.6	121.3	123.2	123.7	127.5
Δ S*(cal.deg.$^{-1}$mole^{-1})	−0.44	−2.40	−3.68	−3.95	−6.45

3-3. Estimation of Errors

(a) Errors in growth curve

The major factors contributing to these are analysis errors, and error in temperature control. The analysis error was estimated to be ± 3% for well crystallized samples, and ± 5% for poorly crystallized samples, and for low mullite concentrations. These estimates were obtained by comparing

duplicate analyses. The error in temperature control was
negligible in comparison with that of the analysis error,
for firing times up to about 4 hours. For longer firing
times the error increased to $\pm$ 10°C, or about $\pm$ 1%, which,
in terms of error in mullite concentration, was about $\pm$ 2-3%.
The combination of these errors gives a maximum total error
of about $\pm$ 6%, on the average.

(b) <u>Error in rate constants</u>

The rate constants were determined by measurement of the
slopes of tangents to the growth curves, which are themselves
subject to an error. An estimate of the resultant error in
R is $\pm$ 20%, and this is the only error involved in the
estimation of K.

(c) <u>Error in Δ H*</u>

The log $(t_{\frac{1}{2}})$ values contained about $\pm$ 10% error. This
arose from personal judgement of the $t_{\frac{1}{2}}$ value from steep
growth curves. The absolute error in Δ H* was thus about
$\pm$ 10-12 K cal/mole. (i.e. $\pm$ 10%).

(d) <u>Error in Δ G*</u>

The K values used to determine Δ G* were themselves
subject to about $\pm$ 20% error. Since this was the only source

of error in estimation of ΔG^*, the absolute error in the latter was about 10–12 K cal.mole^{-1} (i.e. 10%).

(e) Error in ΔS^*

The errors in ΔS^* are very large indeed. The note-worthy feature of the ΔS^* values is that they are all relatively small, and in a narrow range.

REFERENCES – CHAPTER 3

(1)(a) EYRING, H.: J.Chem.Phys. <u>3</u>, 107, (1935).

(b) EVANS, M.G. and POLYANI, M.: Trans.Farad.Soc. <u>31</u>, 875 (1935).

CHAPTER 4

EXPERIMENTAL RESULTS FOR TREATED HALLOYSITES

4-1. Preparation of Clays with Specific Exchange Cations

All hydrogen clay used throughout the present work was prepared by the method of acid ion exchange resin. The resin used, Zeocarb 225, was obtained in its sodium form. It was converted to the hydrogen form by washing with hydrochloric acid, by the method of Vogel (1).

A 2% suspension of the clay sample was made with distilled water, and the required amount of acid resin was added to the suspension, so that the ratio (by weight) of resin to clay was 10:1. The whole mixture was then dispersed with a mechanical stirrer for five minutes, and the clay suspension washed through an 85 mesh sieve into a solution of the chloride of the required cation. The chlorides used were all Analar Reagents. The clay was stirred vigorously with the solution for two minutes with a magnetic follower, then centrifuged out and washed with distilled water until the affluent was neutral. The clay was then extruded, oven dried at $110^{o}C$, prefired up to $650^{o}C$ for 0.5 hours, and fired at the preselected temperature for the required time. This whole procedure was used throughout the present work, except where it is

otherwise stated.

A study was made of the effects on mullite formation of the variation in strength of the cationic solution with which the hydrogen clay was mixed. Solutions of 0.1, 0.01, 10^{-3} and 10^{-5}M copper (II) chloride were made up, and clay samples prepared by mixing with these in the usual way. The prefired extruded rods were fired at 1110°C for 3 hours, and the results obtained from mullite analyses are given in Table 1.

Table 1. Results of Variation in Strength
of Cationic Solution

Treatment	Mean % Mullite (of two samples)
0.1 M Cu^{2+}	38.5 ± 1.0
0.01 M Cu^{2+}	37.0 ± 1.0
10^{-3} M Cu^{2+}	37.5 ± 1.0
10^{-5} M Cu^{2+}	39.0 ± 1.0
resin only	23.0 ± 1.0
no treatment	33.5 ± 1.0

There is no significant variation in the percentage of mullite formed in the clays treated with the various strengths of copper

(II) chloride solution. Throughout the present work it was therefore assumed that the exchange of cations in the solution with hydrogen in exchange positions was independent of the strength of cation solution used. The results in Table 1 show that the rate of mullite formation is greater when the cations in exchange positions on the clay are largely replaced by Cu^{2+}, than in the naturally occurring clay. The occupation of exchange sites is probably connected in some way with mullite formation, since the hydrogen clay produces 10% less mullite than the naturally occurring sample, and we assume that H^+ occupies only exchange sites on the clay.

4-2. Semiquantitative Studies of the Nature and Magnitude of

Effects of Added Impurities

A number of halloysite samples were prepared, in which as many of the exchangeable cations as possible were replaced by a single metal species. Samples were prepared containing the following cations:

$$K^+ \quad Na^{2+} \quad Ca^{2+} \quad Ba^{2+} \quad Cu^{2+} \quad Ni^{2+} \quad Co^{2+} \quad Mg^{2+} \quad Mn^{2+}$$
$$Hg^{2+} \quad Cd^{2+} \quad Sr^{2+} \quad Sn^{2+} \quad and \quad Fe^{3+}.$$
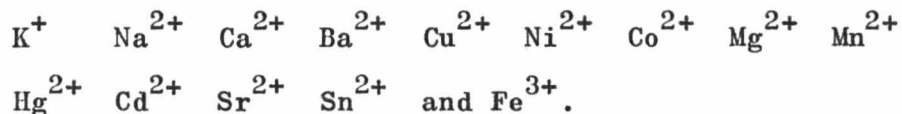
The samples were extruded, prefired to $650^{o}C$ for 0.5 hour, fired isothermally at $1110^{o}C$ for 3 hours, and analysed for mullite.

The results are given in the middle column in Table 2, and
show a large variation in the percentage of mullite formed.

Table 2. Mullite Analyses on Cation Saturated Halloysites

Cation	% Mullite (Te Puke Halloysite)	% Mullite (Takaka Halloysite)
K^+	35.0	25.0
Na^+	37.0	35.0
Ca^{2+}	24.0	25.0
Ba^{2+}	35.0	0.0
Cu^{2+}	45.0	49.0
Ni^{2+}	41.0	31.0
Co^{2+}	41.0	20.0
Mg^{2+}	46.0	26.5
Mn^{2+}	43.0	72.5
Hg^{2+}	28.0	24.0
Cd^{2+}	22.0	61.0
Sr^{2+}	17.0	35.0
Sn^{2+}	42.0	
Fe^{3+}	41.0	25.5
H^+	23.0	24.0

The results in the right hand column of Table 2 are those
obtained by MacKenzie (2) by similar treatments of an halloysite
mineral from Takaka, New Zealand, the firing being performed at
1100°C for 4 hours.

There are large differences between the rates of mullite formation resulting from similar treatments on the two different clays. These results suggest that any mechanistic treatment of mullite formation in cation saturated clays is likely to be valid only for the clay under investigation.

The two clays were then treated with saturated solutions of the chlorides of the cations listed previously in this section. The resultant clays were centrifuged out, but not washed. The treatment was otherwise the same as usual, and it was assumed that, for the reaction in question, the clay was effectively mixed with the powdered oxide of the cation, as well as having the cation adsorbed on exchange sites of the clay. The results of mullite formation are given in Table 3, the Te Puke samples were fired for 3 hours at $1110^{o}C$, the Takaka samples for 4 hours at $1100^{o}C$.

The results for the two clays, under the same treatment are the same (except for Mg^{2+}), within the range of experimental error, although there were large differences between results for the similar treatments in Table 2. This may imply that the addition of such a large amount of impurity would have basically the same effect on mullite formation in all clays which are largely halloysitic. If this is so, it would in principle be

Table 3. Mullite Analyses on Halloysites Mixed
with Cation-Oxides

Cation	% Mullite (Te Puke Halloysite)	% Mullite (Takaka Halloysite)
K^+	10	17
Na^+	30	
Ca^{2+}	39	
Ba^{2+}	34	
Cu^{2+}	31	34
Ni^{2+}	10	10
Co^{2+}	18	18
Mg^{2+}	16	35
Mn^{2+}	38	41
Hg^{2+}	20	
Cd^{2+}	39	
Sr^{2+}	27	
Sn^{2+}	25	
Fe^{3+}	33	

easier to fit in with a generalized mechanism of mullite formation
under these conditions, covering other systems as well.   The
results of Table 2 suggest, however, that this is difficult when
the added impurity is associated only with exchange sites.

56.

4-3. Mullite Growth Curves from Cation Saturated Halloysites

Sodium, calcium, manganese, iron (III) and copper were chosen as cations for the detailed study of the effects of cation exchange on mullite formation. Samples were prepared in which as many of the exchangeable cations as possible were replaced by the single metal species under investigation. Figures 4A, 4B, 4C, 4D and 4E give the growth curves for the cation halloysites, and the reduced growth curves are shown in Fig. 4F, superimposed on that of the untreated halloysite. The background line in Fig. 4F is the line of nearest fit from Fig. 3B. The superimposition suggests a similar mechanism of mullite formation in all samples.

4-4. Thermodynamics of Mullite Formation from the Cation Saturated
Halloysites

The thermodynamic functions for the reaction were obtained by applying Eyring Rate Theory as discussed in Section 3-2.

Table 4 gives the thermodynamic functions, and a discussion of the results will be given in the next chapter.

4-5. Errors

The errors in k and ΔG^* have the same magnitudes as the errors for the untreated clay, and the error in ΔS^* is still very large. ΔH^* is evaluated from only two or three points on

Table 4.

A. Sodium Halloysite			
T (^{o}C)	1170	1110	
k (sec.$^{-1}$)	3.92×10^{-6}	5.16×10^{-6}	
Δ H*(k cal.mole^{-1})	51	51	
Δ G*(k cal.mole^{-1})	125	119	
Δ S*(cal.deg.$^{-1}$mole^{-1})	−51.3	−49.0	

B. Calcium Halloysite			
T (^{o}C)	1170	1110	
k (sec.$^{-1}$)	5.06×10^{-6}	3.58×10^{-6}	
Δ H*(k cal.mole^{-1})	78	78	
Δ G*(k cal.mole^{-1})	124	120	
Δ S*(cal.deg.$^{-1}$mole^{-1})	−31.9	−30.4	

C. Manganese Halloysite			
T (^{o}C)	1110	1050	1020
k (sec.$^{-1}$)	8.00×10^{-6}	4.95×10^{-6}	3.84×10^{-6}
Δ H*(k cal.mole^{-1})	83	83	83
Δ G*(k cal.mole^{-1})	118	114	111
Δ S*(cal.deg.$^{-1}$mole^{-1})	−25.3	−23.4	−21.6

D. Iron (III) Halloysite			
T (^{o}C)	1170	1110	
k (sec.$^{-1}$)	4.50×10^{-6}	2.53×10^{-6}	
Δ H*(k cal.mole^{-1})	60	60	
Δ G*(k cal.mole^{-1})	124	121	
Δ S*(cal.deg.$^{-1}$mole^{-1})	−44.4	−44.0	

E. Copper Halloysite			
T (^{o}C)	1110	1080	1050
k (sec.$^{-1}$)	5.17×10^{-6}	4.11×10^{-6}	4.11×10^{-6}
Δ H*(k cal.mole^{-1})	106	106	106
Δ G*(k cal.mole^{-1})	119	117	114
Δ S*(cal.deg.$^{-1}$mole^{-1})	−9.4	−8.1	−6.0

the graph of log $t_{\frac{1}{2}}$ versus $1/T$, and the error in $\triangle$ H* will thus be larger than the $\pm 10\%$ allowed for in section 3-3 for the naturally occurring sample, when there were five points on the graph. A conservative estimate of this error is $\pm 20\%$.

REFERENCES — CHAPTER 4

(1) VOGEL, A.I.: "A Textbook of Quantitative Inorganic Analysis", p.712 (3rd Ed.) Longmans.

(2) MACKENZIE, K.J.D.: "The Kinetics and Mechanism of the High Temperature Solid State Reactions of Kaolinite Minerals", M.Sc. Thesis, V.U.W., p.68 (1964).
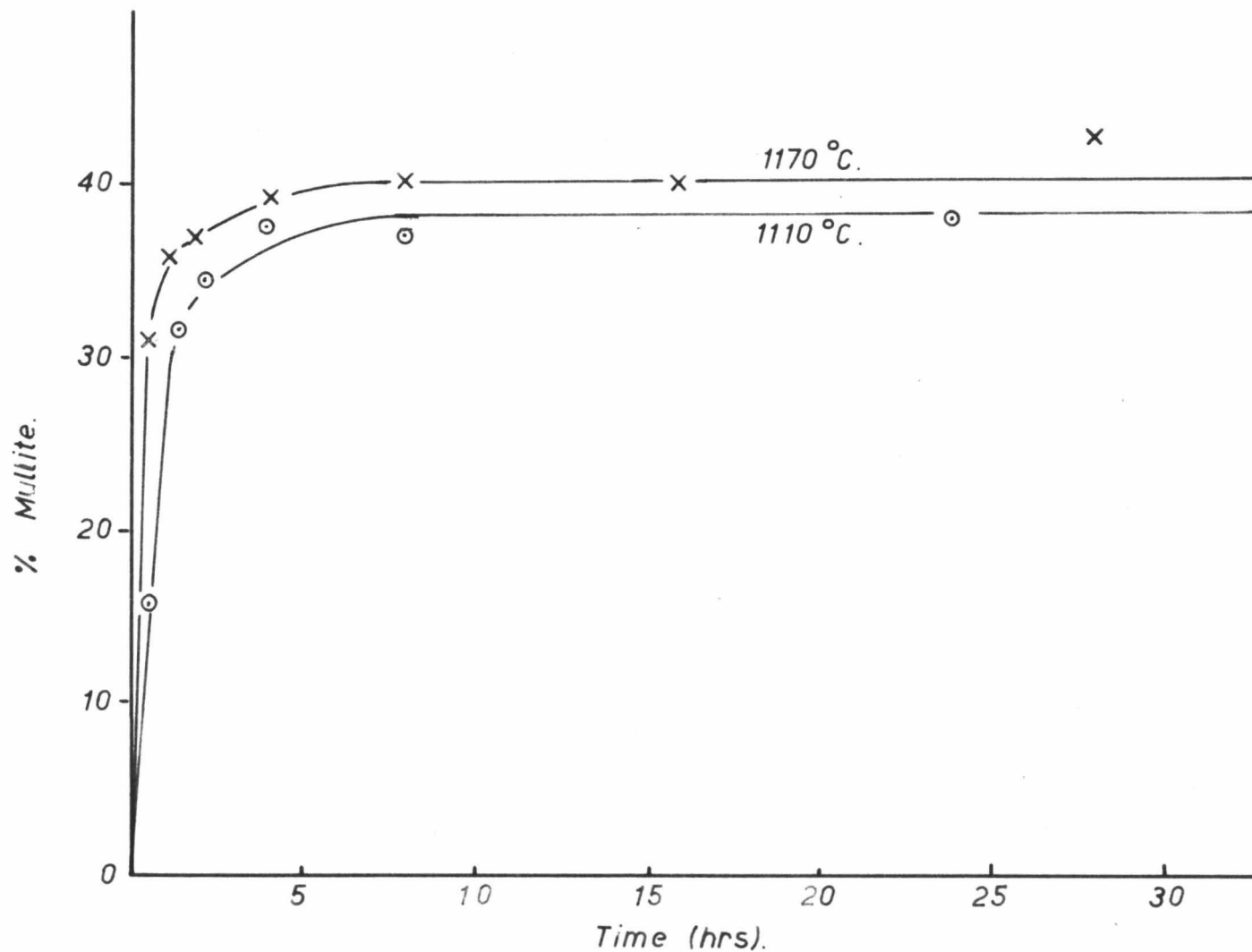
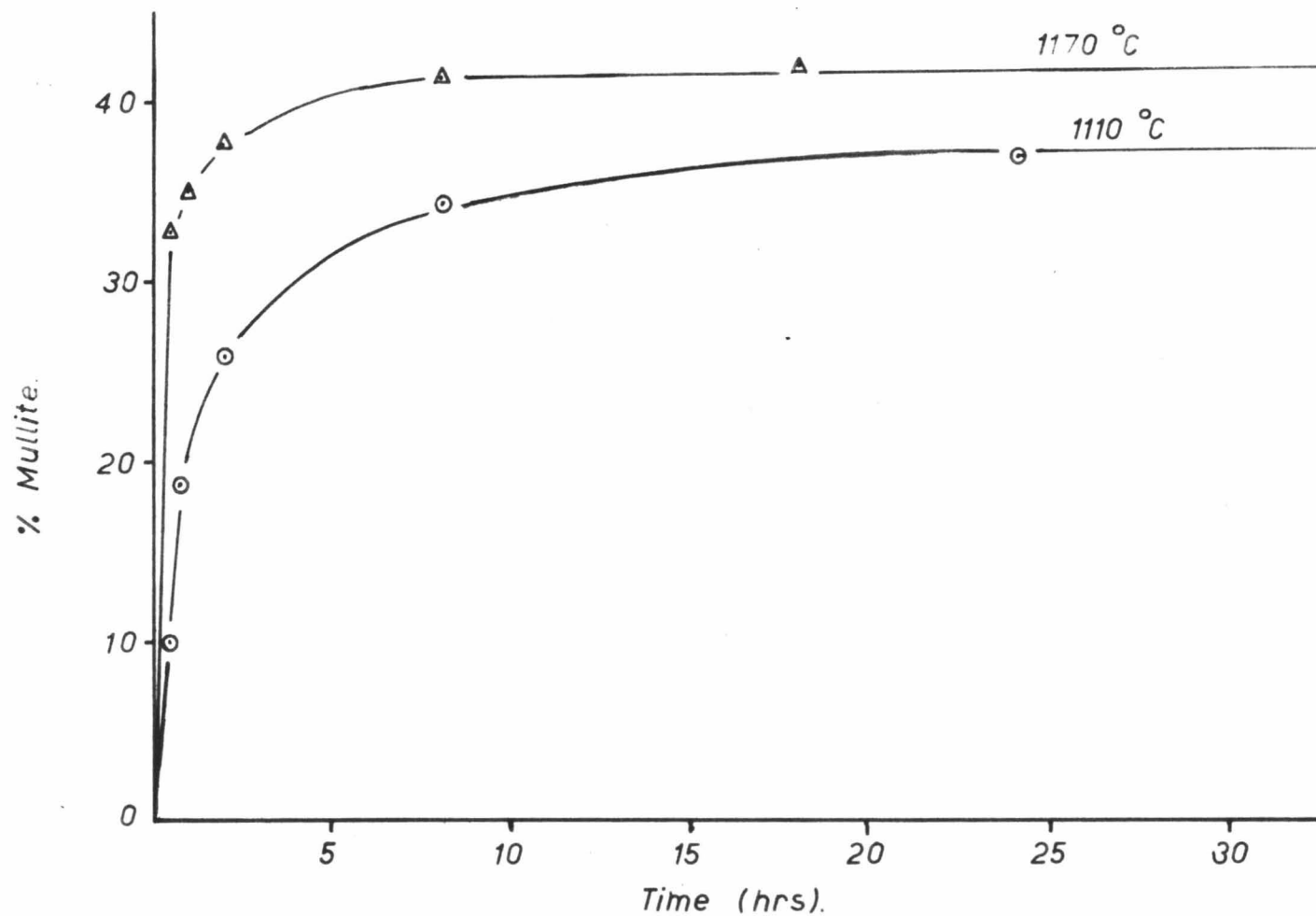Fig. 4A. Mullite growth curves from Sodium Halloysite.

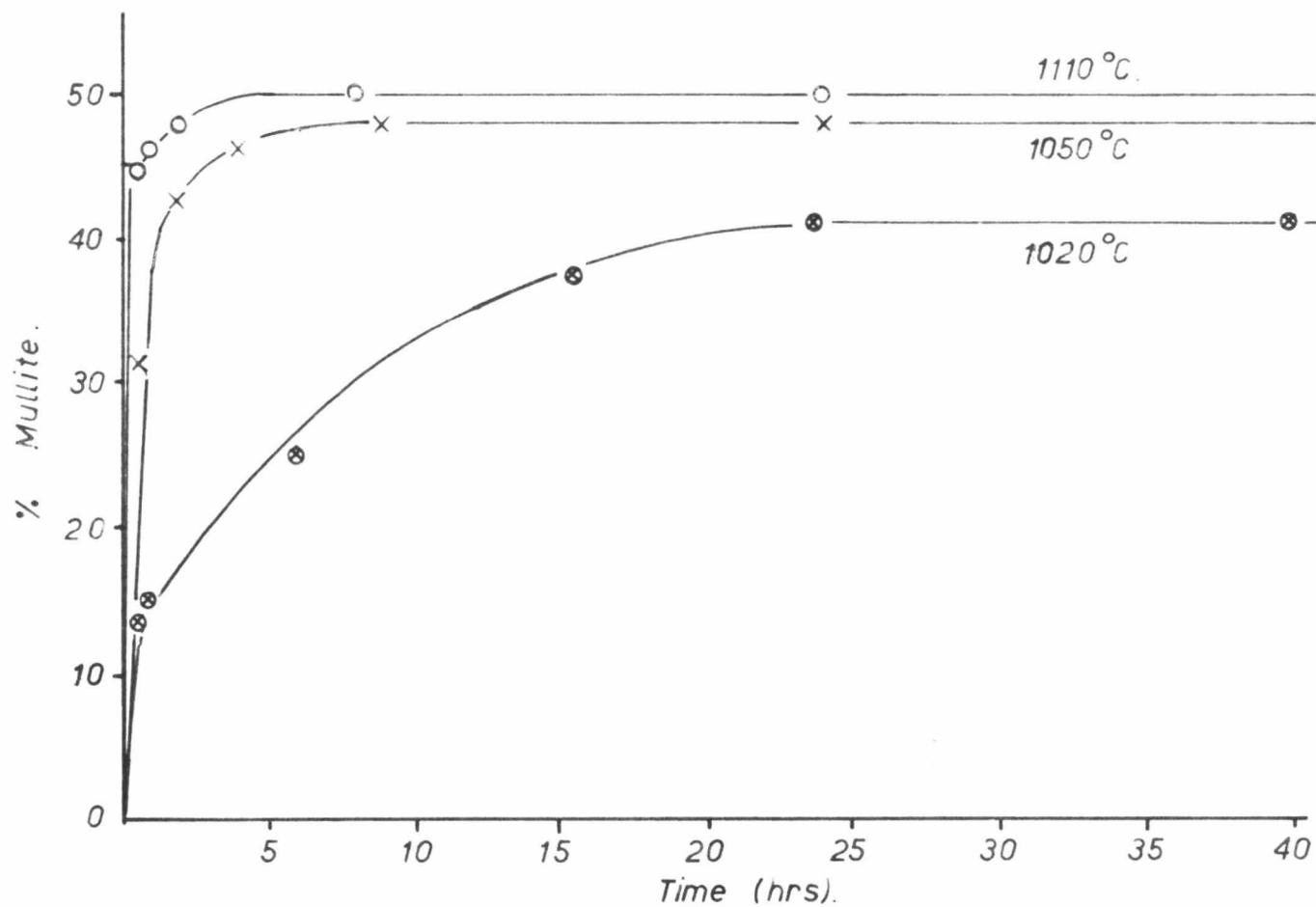Fig. 4 B. Mullite growth curves from Calcium Halloysite.
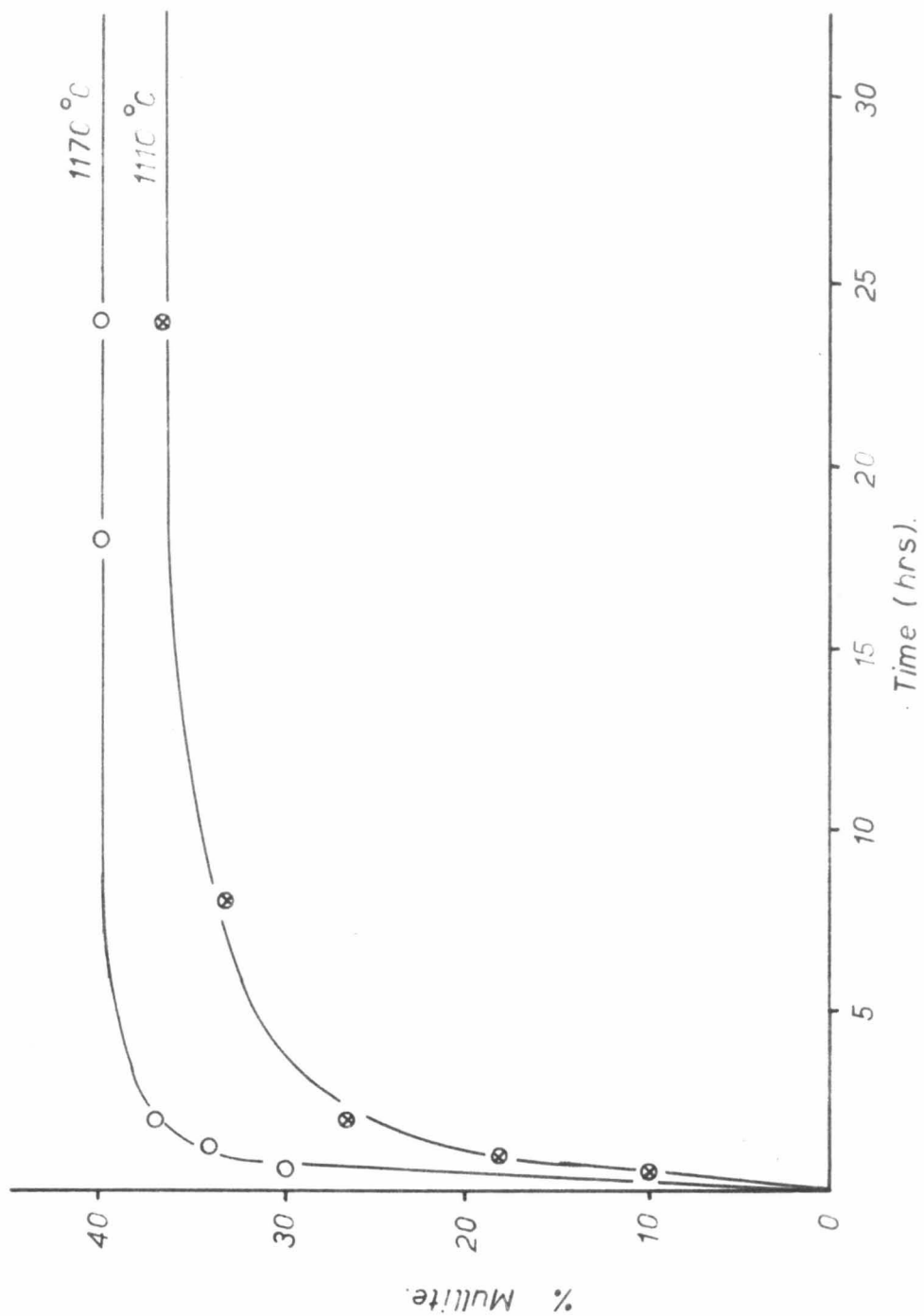
Fig. 4 C. Mullite growth curves from Manganese Halloysite.
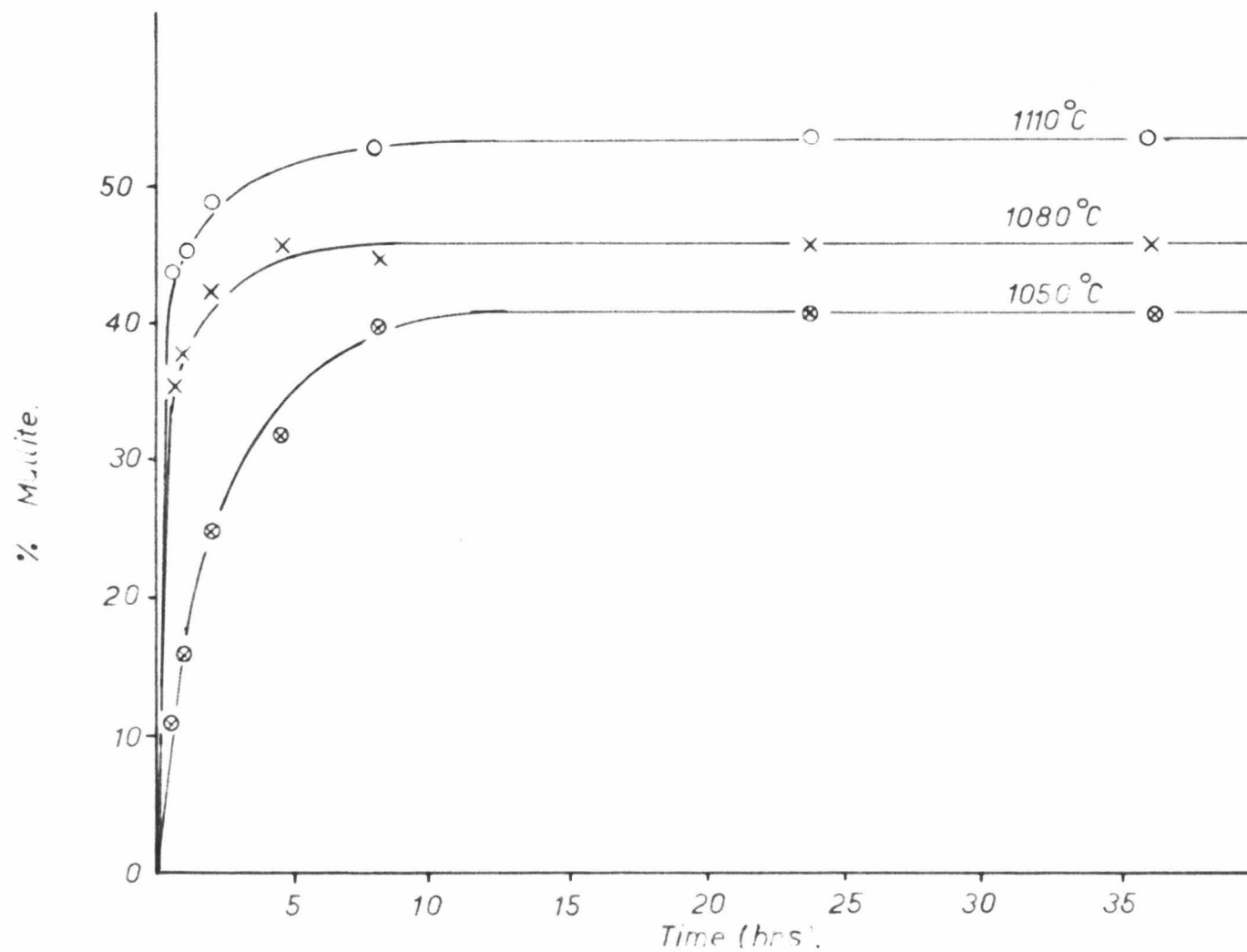
62

Fig. 4D. Mullite growth curves for Iron (III) Halloysite.

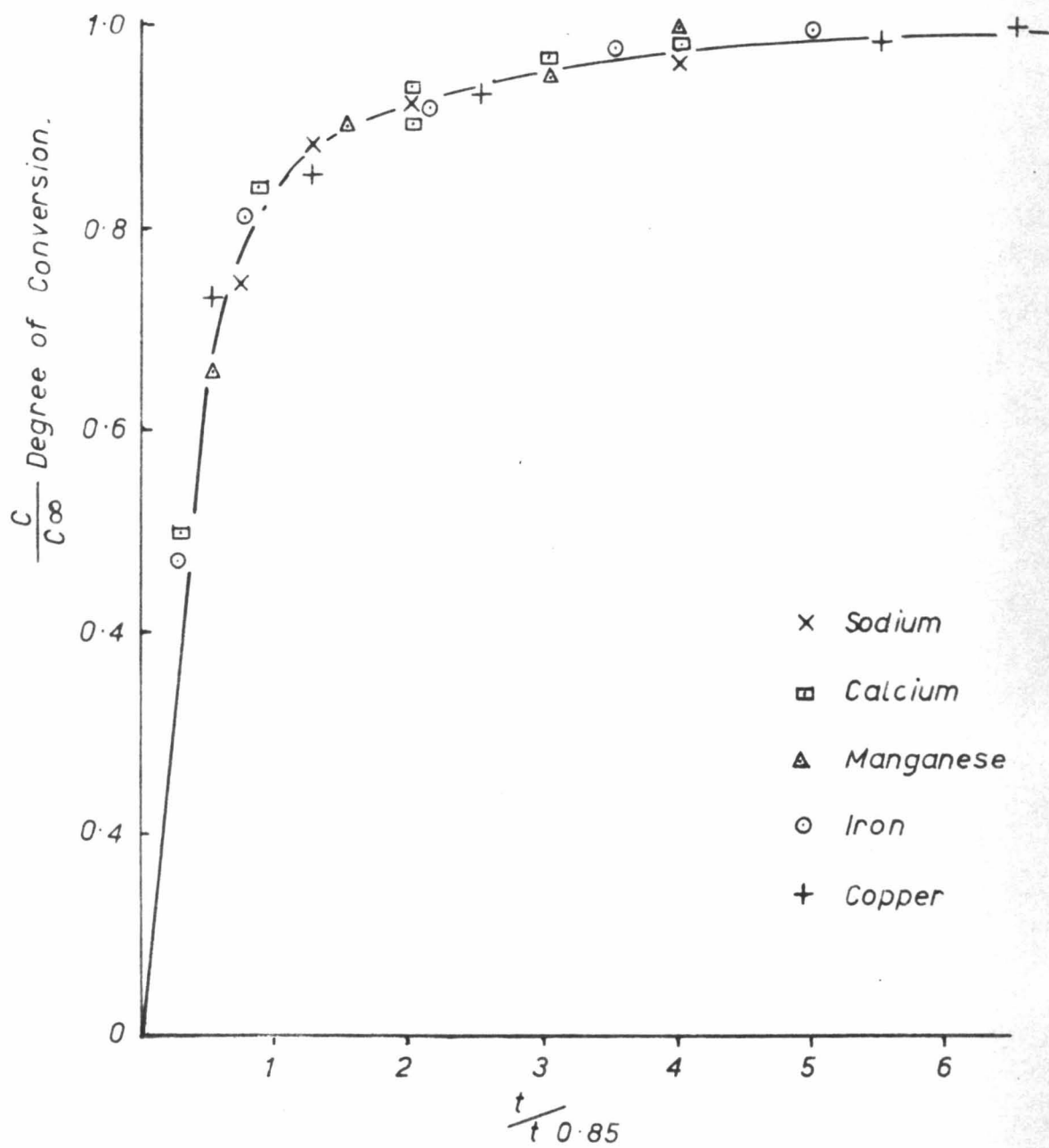Fig. 4 E. Mullite growth curves from Copper Halloysite

64

Fig. 4F. Reduced growth curve

CHAPTER 5

DISCUSSION OF THE EXPERIMENTAL RESULTS

The presence of certain cations has been found to lower the temperature at which mullite develops.   From the results of this work there appears to be no systematic correlation between the effects of a mineralizing ion and its valence, nor any definite association between the observed effects and the ionic radii of the exchanged cations.   According to Wahl and Grim (1), it is probable that the presence of some ions in chemical systems causes a lowering of the melting temperature of the heated sample, thus allowing the initial crystallization of the high temperature phases to occur at a lower temperature than that normally considered essential.

5-1. Discussion of the Growth Curves

Table 1 gives a summary of the effects of cationic impurities on the temperature at which detectable mullite first develops. The maximum percentages of mullite formed from a given cation clay are also recorded in Table 1.

An interpretation of the results in Table 1 is now given. Cu^{2+} and Mn^{2+} significantly lower the threshold temperature of

Table 1. Summary of the Effects of Cationic

Impurities on Mullite Formation.

Additive	Effect on Mullite Formation	C_∞ =Maximum % Mullite Formed
Cu^{2+}	lowered $\sim 60^{\circ}C$	54
Fe^{3+}	none	40
Na^{+}	lowered $\sim 30^{\circ}C$	40
Mn^{2+}	lowered $60 - 90^{\circ}C$	50
Ca^{2+}	none	42
None		50

mullite formation, while leaving the value of C_∞ virtually

unchanged.   The cations would be expected to facilitate mullite

formation by allowing a reaction path of lower energy than usual.

The structures of the phases formed are, however, possibly not

altered to such an extent as to give rise to amounts of detectable

mullite different from those formed from the naturally occurring

halloysite.

Fe^{3+} has no significant effect on the temperature at which

mullite is initially formed, and the C_∞ for iron (III) halloysite

is 10% lower than for the untreated clay.   The texture of the

mullite peaks from iron (III) halloysite was observed to be diffuse, especially at low firing times. During the ion exchange process, a smaller amount of Fe^{3+} will be required to satisfy the charge neutrality, than if the ion had a lower valence. If Fe^{3+} ions were to provide a mechanism of nucleus formation, then the reaction rate would fall as the availability of Fe^{3+} decreases, and this would occur sooner with Fe^{3+} than with uni- or di-valent ions. The low C_∞ may thus be interpreted in terms of low availability of Fe^{3+}.

The texture of mullite peaks from calcium and sodium halloysites was also found to be rather diffuse. This indicated that the mullite was poorly crystallized, or in the form of small nuclei just detectable to the X-ray.

Table 2 gives the ionic radii of the ions under investigation, after Pauling (2).

Table 2. Ionic Radii after Pauling (2).

Mn^+	γMn^+
Na^+	0.95
Ca^{2+}	0.99
Mn^{2+}	0.80
Cu^{2+}	0.92
Fe^{3+}	0.53
Al^{3+}	0.50
Si^{4+}	0.41

Both Na^+ and Ca^{2+} differ considerably in size, and formal charge, from the cations which form the major part of the lattice (i.e. Al^{3+} and Si^{4+}). The presence of either of these in the lattice would therefore be expected to give rise to some form of dislocation. The defects so produced would then provide nuclei for mullite formation, but the extensive dislocation could cause the formation of poorly ordered mullite.

5-2. Discussion of the Thermodynamic Functions

MacKenzie (5) found no significant variation in the thermo-dynamic functions for mullite formation in three kaolinite minerals, and a large variation in the values of rate contents. The present author has evaluated thermodynamic functions and finds that rate constants and Δ G* values are independent of the starting material, while Δ H* and Δ S* are dependent on the impurity content of the sample being studied.

(a) Enthalpies of Activation

The Δ H* values obtained in the present study vary from 50 to 120 k cal/mole. Lundin (3) obtained energies of activation for mullite formation within the range 190-220 k cal. mole^{-1}, and Budnikov (4), by a chemical method, found a Δ H* of about 50 k cal. mole^{-1}. Δ H* values of MacKenzie (5), who studied mullite formation in an halloysite, the

copper saturated halloysite, and a kaolinite, were in the range $(87 - 96 \pm 20)$ k cal. mole^{-1}. The large variation in the Δ H* values evaluated by the different workers using methods subject to errors small enough to make this variation significant, suggests that the energy of activation must bear some relation to the impurity content of the clay under investigation.

The energies of activation obtained by the present author are of the order of diffusion process energies. The lattice probably therefore undergoes a gradual rearrangement to form mullite at high temperatures, rather than undergoing a sudden collapse. Δ H* is a measure of the difference in energy between the ground state of the reactants (presumably the spinel form), and the transition state leading to mullite formation.

The Δ H* values found in the present study appear to lie in three ranges:

(a) $50 - 60$ $(\pm 6 - 8)$ k cal. mole^{-1}

    e.g. Sodium Halloysite Δ H* = 51 k cal.mole^{-1}

        Iron (III) Halloysite Δ H* = 60 k cal.mole^{-1}

(b) $75 - 85$ $(\pm 8 - 10)$ k cal. mole^{-1}

    e.g. Calcium Halloysite Δ H* = 78 k cal.mole^{-1}

        Manganese Halloysite Δ H* = 83 k cal.mole^{-1}

(c)   100 - 120 ($\pm$ 10 - 12) k cal.mole^{-1}

e.g. Copper Halloysite $\triangle$ H* = 106 k cal.mole^{-1}

Untreated Halloysite $\triangle$ H* = 118 k cal.mole^{-1}

The divisions may be fortuitous, since $\triangle$ H* depends on two quantities: the energy of the ground state, and the energy of the transition state. A low $\triangle$ H*, for instance, may result from a low energy transition state or a high energy ground state, or both.

Fe^{3+} is a small, highly charged ion, unlike the large, low charged Na^{+}. The low $\triangle$ H* values in the sodium and iron (III) halloysites would therefore be expected to have arisen for rather different reasons. Fe^{3+} is probably relatively mobile, as a result of its size. Hence if diffusion is a rate controlling process in mullite formation, the presence of Fe^{3+} ions might be expected to facilitate the reaction. From its size, Na^{+}, on the other hand, may give rise to the formation of defects which provide nuclei for mullite formation.

Ca^{2+} and Mn^{2+} are comparable in formal size and charge, but from the different properties of the cations we might expect that the reasons for the similar $\triangle$ H* values are not the same for the two clays.

$\triangle$ H* appears to be unaffected, within the range of experimental error, by the addition of Cu^{2+}. MacKenzie (5) observed a similar relation between the $\triangle$ H* values of mullite formation from an halloysite ($\triangle$ H* = 93 k cal.mole^{-1}) and its copper saturated form ($\triangle$ H* = 96 k cal.mole^{-1}).

(b) Free Energies of Activation

$\triangle$ G* values obtained from the kinetic study lie within the relatively narrow range of (120 $\pm$ 15) k cal.mole^{-1}, so that the free energy barrier to all reactions producing mullite was approximately the same.

(c) Entropies of Activation

The entropies of activation are all negative, indicating an increase of order in the transition state. The magnitudes of the $\triangle$ S* are small, which suggests that there is no extensive rearrangement of the lattice. Migration of silicon and aluminium ions from random positions to the aluminium rich spinel and the silicon rich cristobalite regions explains the sign of $\triangle$ S*. The $\triangle$ S* values are in the range (0 to - 50) cal.deg.$^{-1}$mole^{-1}.

5-3. Mullite Formation

McVay (6) suggests that the mullite phase is formed by three

processes:

(i)   In kaolinite by direct dissociation and crystal
       growth.

(ii)   By recrystallisation.

(iii) During cooling.

The reaction mechanisms may be different for each of these methods
of formation.

Taylor (7) (1962) has suggested an inhomogeneous mechanism
for mullite formation.   The oxygen lattice is assumed fixed, so
that cation migration occurs giving rise to aluminium rich regions
(which become spinel), and silicon rich regions (which become
cristobalite).   The mechanism appears reasonable on chemical
grounds, although Taylor does not attempt to describe in any
detail the processes involved.

5-4. Mathematical Treatment of the Experimental Growth Curves

The rates of the following processes would be expected to
influence the rate of mullite formation:

(a)   cation migration

(b)   nucleation of mullite

(c)   crystal growth.

Since visual observations of the product phase are restricted to

three dimensional growth, it is assumed that the reacting particles and the product nuclei are spherical.

Jander (8)(1927) published a model of the kinetics of solid state reactions, in which he considered a sphere of radius r, the complete surface of which was reacting with other spheres, and developing a reaction product of thickness y. The reaction was assumed to be diffusion controlled, and the rate of thickening of the reaction product was assumed to be inversely proportional to its thickness:

$$\frac{dy}{dt} = \frac{k}{y} \qquad \qquad \dots\dots(5, 1)$$

Integration of (5, 1) gives

$$y^2 = 2kt \qquad \qquad \dots\dots(5, 2)$$

The volume, v, of unreacted material at time t is:

$$v = \frac{4}{3} \pi (r - y)^3 \qquad \qquad \dots\dots(5, 3)$$

$$= \frac{4}{3} \pi r^3 (1 - x) \qquad \qquad \dots\dots(5, 4)$$

where x = fraction of the original sphere which has reacted. Equating (5, 3) and (5, 4) gives:

$$y = r\left[1 - (1 - x)^{\frac{1}{3}} \right] \qquad \qquad \dots\dots(5, 5)$$

and substitution of (5, 5) in (5, 2) yields equation (5, 6):

$$\left[1 - (1 - x)^{\frac{1}{3}} \right]^2 = \frac{2kt}{r^2} = Kt \qquad \qquad \ldots \ldots (5, 6)$$

A plot of $\left[1 - (1 - x)^{\frac{1}{3}} \right]^2$ versus t should therefore be a straight line.   This is in fact found to be the case up to 80% conversion of mullite (see Fig. 5A).   Equation (5, 6) may be used to plot a theoretical curve of $\frac{C}{C_\infty}$ versus t, and this is shown in Fig. 5C.   There is no agreement between theory and experiment until about 80% conversion.   There are two oversimplifications in Jander's model:

(a)   Equation (5, 1) is for the reaction of a plane surface.
The rate of thickening of a spherical shell of reaction
product must depend on the ratio of areas of outer to inner
surfaces.   The analysis would therefore be expected to hold
only for small values of x, where the ratio is near unity.

(b)   Equating (5, 3) and (5, 4) implies that the volumes of
equivalents of reactant and reaction product are equal.
This is not generally the case.

The results of more sophisticated theoretical treatments of the kinetics of growth of precipitates from solid solutions can usually be reduced to the general form (9):

$$y = 1 - \exp - (t/k)^n \qquad \qquad \ldots \ldots (5, 7)$$

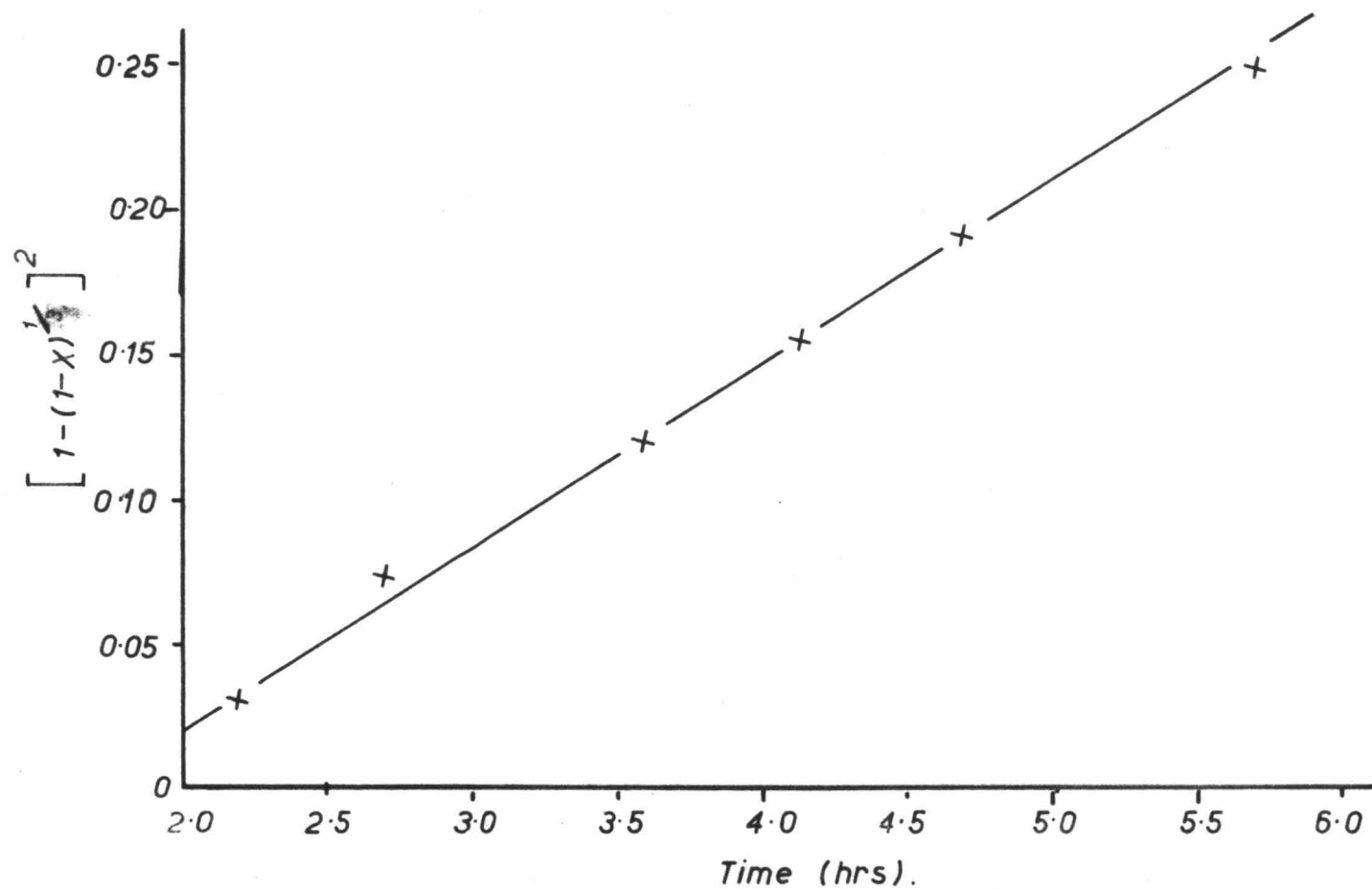where y = fraction precipitated in time t, k and n are constants.

Fig. 5A. Graph of $\left[1-(1-X)^{\frac{1}{3}}\right]^2$ versus time.

In deriving equations of this type, the procedure has usually been to calculate the rate of growth of one particle of the new phase as a function of time, sum over all particles present in unit volume of the solid solution, and then allow for the reduction in reaction rate consequent upon the impingement of the zones of the parent phase depleted of reactant. A treatment by Burke (9) considers the case of spherically precipitated particles, and makes the following assumptions:

(1) The reaction proceeds by the growth of a fixed number of nuclei, all of which are formed at $t = 0$.

(2) The matrix is initially homogeneous.

(3) The distribution of nuclei is random.

(4) The rate of growth is determined by the rate of diffusion of solute in the matrix, and the diffusion coefficient, D, is independent of concentration.

By solution of Fick's equation (5, 8):

$$\frac{\partial c}{\partial t} = D \left[\frac{\partial^2 c}{\partial r^2} + \frac{2}{r} \frac{\partial c}{\partial r} \right] \qquad \ldots \ldots (5, 8)$$

assuming a quasi-stationary state, the following equation is obtained as the rate equation for this particular model:

$$\frac{1}{2}\ln \left[\frac{1 + y^{\frac{1}{3}} + y^{\frac{2}{3}}}{(y^{\frac{1}{3}} - 1)^2} \right] + 3 \left[\tan^{-1} - (\frac{2y^{\frac{1}{3}} + 1}{3}) - \frac{5\pi}{6} \right]$$

$$= 3 \beta y^{\frac{2}{3}} t \qquad \ldots \ldots (5, 9)$$

where y = fraction of total precipitation occurred at time t

β , γ are assumed constant.

A plot of the left hand side of equation (5, 9) versus t should be a straight line. This is in fact found to be the case (see Fig. 5B). Although this model provides a description of the results it is not necessarily the only valid interpretation.

Jacobs and Tompkins (10) have proposed models for precipitation from solid solutions where crystal growth is assumed to be the rate controlling factor, and nucleation may affect the rate to a small but significant extent. It may be deduced from the laws of nucleus formation that for nucleation involving a single step, the probability that a single molecule will decompose to form a nucleus is (10):

$$k_1 = \gamma e^{\frac{-\Delta G_1}{Rt}} \qquad \dots\dots(5, 10)$$

where γ = frequency of the lattice vibrations

ΔG_1 = free energy of activation for nucleus formation.

If there are No potential nuclei forming sites, the rate of nucleus formation is
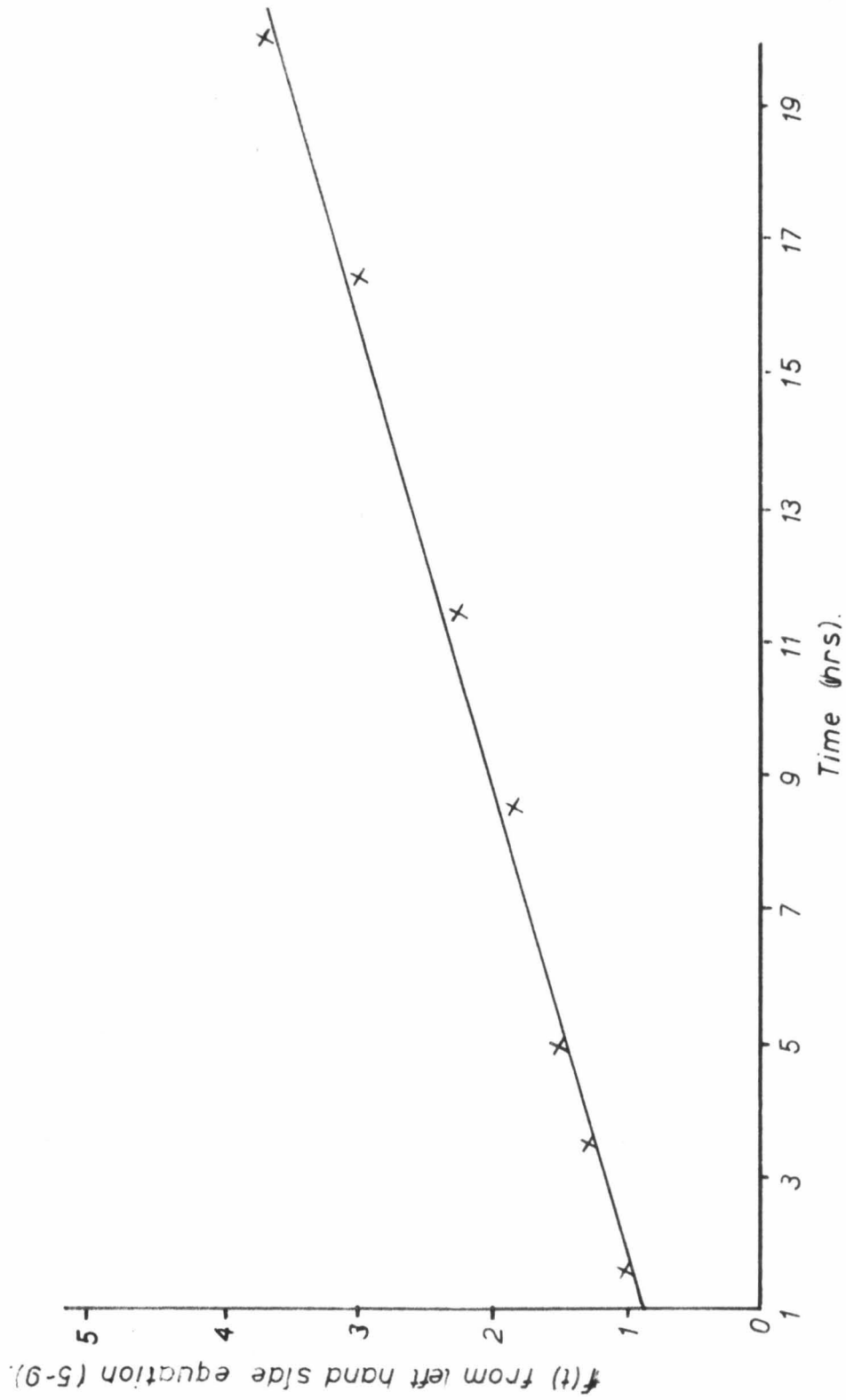
$$\frac{dN}{dt} = k_1(No - N) \qquad \dots\dots(5, 11)$$

Fig. 5.B. Plot of left hand side of equation (5-9). versus time.

Time (hrs).

f(t) from left hand side equation (5-9).

where N = number of nuclei at time t.

Integration of (5, 11) yields

$$N = No(1 - e^{-k_1 t})$$ .....(5, 12)

so $$\frac{dN}{dt} = k_1 No\, e^{-k_1 t}$$ .....(5, 13)

If N = No, nucleation is instantaneous.   Otherwise nucleation
obeys the exponential law of equation (5, 13).

The situation is here examined where the rate of nucleation
is assumed to be so rapid that it is instantaneous.   Consider a
crystal of A(s) in which the surface material undergoes rapid
decomposition to form a layer of B(s).   There is then a complete
interface between product and reactant, at which further reaction
proceeds.   If ΔG_2^* is the free energy of activation for interface
reaction, and if the number of molecules at the interface is N,
then:

$$-\frac{dN}{dt} = N\gamma\, e^{\frac{-\Delta G_2^*}{Rt}}$$ .....(5,14)

or $$-\frac{dN}{dt} = S_2 N\gamma\, e^{\frac{-E_2^*}{Rt}}$$ .....(5, 15)

This is the Polyani-Wigner equation.   A constant rate of reaction
would be expected for a constant area of interface, and linear rates
are observed during the early stages of the reaction, in agreement

with this prediction.

We now replace N by $A\bar{N}$, where $\bar{N}$ = number of molecules per unit area of interface. Then

$$- \frac{dN}{dt} = S_2 \gamma \bar{N}A\,e^{-\frac{E_2^*}{Rt}} \qquad \ldots\ldots(5,\ 16)$$

$$= k_2 A \qquad \ldots\ldots(5,\ 17)$$

k_2 = rate of reaction per unit area

A = superficial area of interface.

If the reactant is assumed to consist of a uniform aggregate of small crystals, and the interface is represented by a contracting sphere, then if the spherical particles were of initial radius a, the fraction decomposed at time $t, \alpha \frac{= C}{C_\infty}$, would be:

$$= \frac{\frac{4\pi}{3} a^3 - \frac{4\pi}{3} (a - k_2 t)^3}{\frac{4\pi}{3} a^3} \qquad \ldots\ldots(5,\ 18)$$

$$\alpha = 1 - \left(\frac{1 - k_2 t}{a}\right)^3 \qquad \ldots\ldots(5,\ 19)$$

$$\text{or } 1 - \frac{k_2 t}{a} = (1 - \alpha)^{\frac{1}{3}} \qquad \ldots\ldots(5,\ 20)$$

Equation $(5,\ 20)$ can be used to plot a theoretical curve of $\frac{C}{C_\infty}$ versus t, shown in Fig. 5C. Agreement is good up to 80% conversion of mullite, after which the predicted $\frac{C}{C_\infty}$ values are too high. This would be expected from the approximation of constant radius.
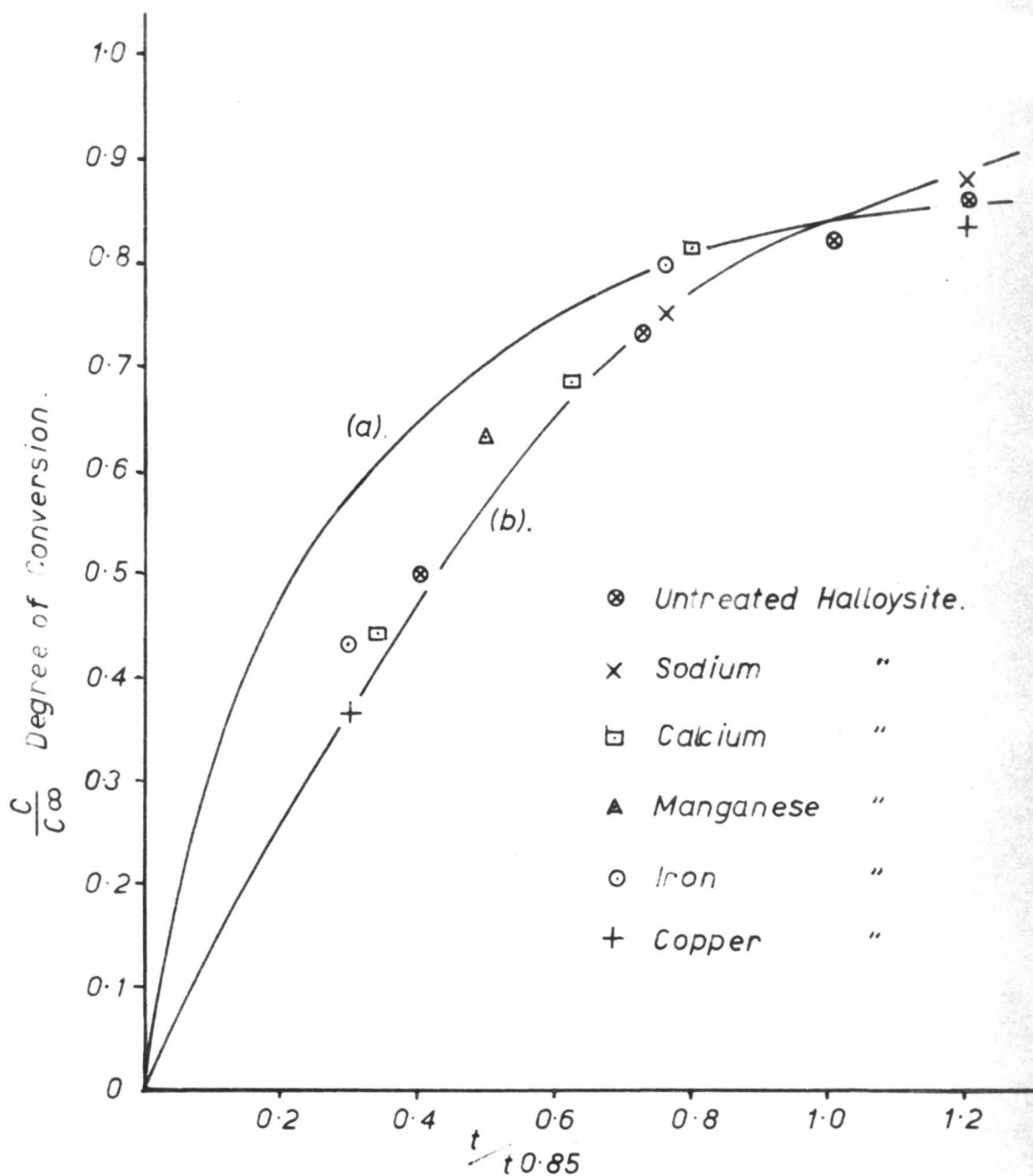
Fig. 5 C.   Comparison of theoretical growth curves with experimental results. (a) After Jander (8), (b) After Jacobs & Tompkins (10)

A refinement may now be introduced (10) by assuming that the nucleation rate affects the overall rate of precipitation. The nucleation of particles is assumed to obey an exponential law. A mathematical treatment (10) yields the following expression for the fraction decomposed (α):

$$1 - \alpha(t) = e^{-k_1 t} \left[B(1 - e^{k_1 t_1}) - 1 \right] = A e^{-k_1 t} \quad \ldots (5, 21)$$

where B, k_1, t_1 are constants for any given substance, particle size, and temperature. A plot of $\log (1 - \alpha)$ versus t would thus be expected to be linear, and this is found to be the case (see Fig. 5D).

5-5. Conclusion

The kinetics of mullite formation from metakaolinite appear to be consistent with rapid exponential nucleation of mullite from the spinel phase, and rapid crystal growth. The results at latter stages of the reaction suggest that a simple diffusion law is obeyed.

The addition of iron (III), copper, manganese, calcium and sodium to give the respective cation-saturated halloysites lowers, or leaves unchanged the threshold temperature for mullite formation. The experimental free energies of activation and rate constants are similar for all samples studied, but the entropies
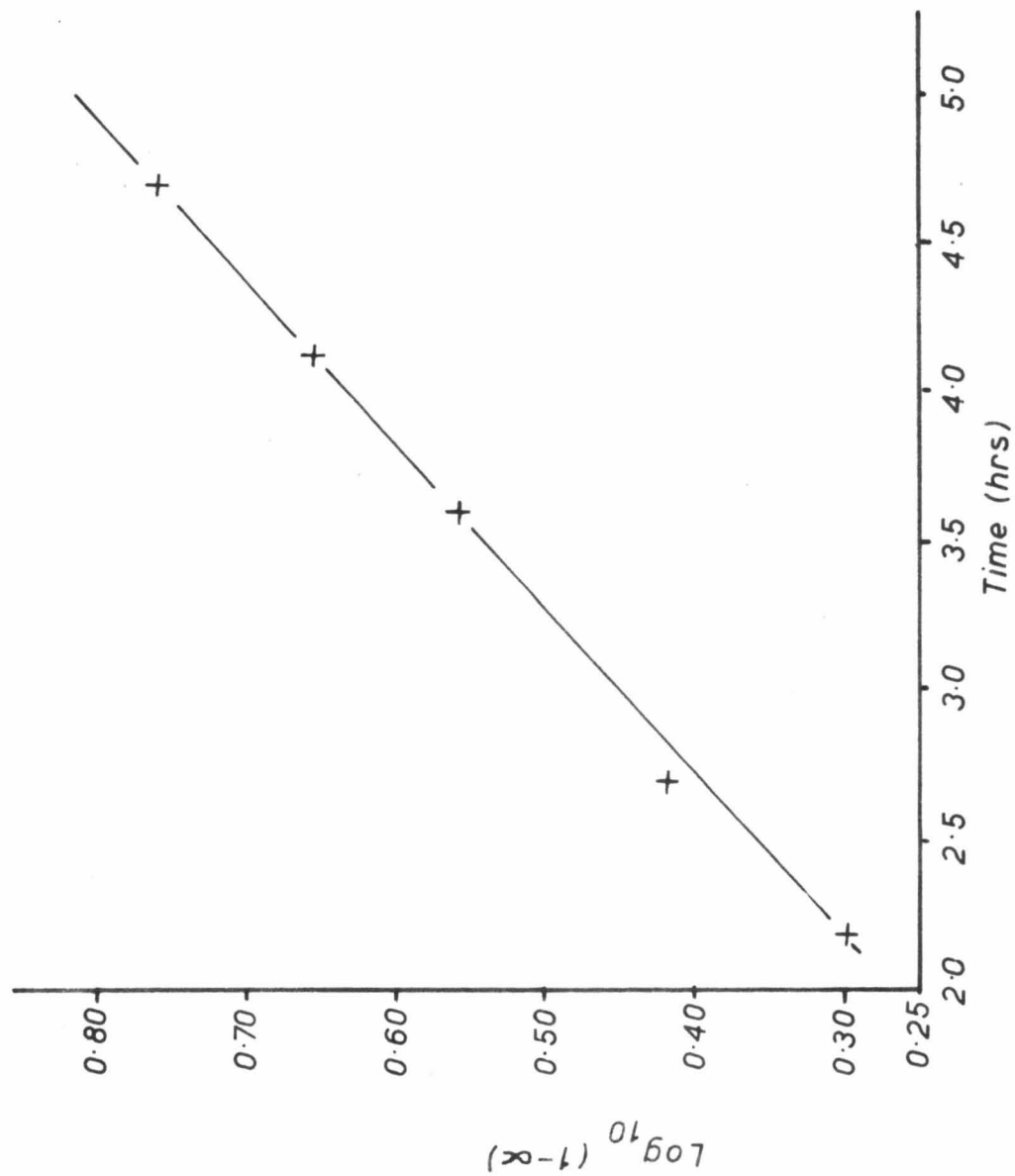
Fig. 5D. Plot of $\log_{10}(1-\alpha)$. versus time.

and enthalpies of activation depend on the impurity content of the starting material.

The added impurity is present in such minute concentrations that it would not be expected to affect the growth rate of mullite nuclei to any appreciable extent. Since nucleation would be expected to occur at sites of disorder, if these sites are assumed to exist largely on the surfaces of the double layer halloysite structure, then the cations would be expected to influence the rate of nucleation. The entropy of activation for mullite formation would be related to the rate of nucleation of mullite. The $\triangle$ S* values are given in Table 3.

Table 3. Entropies of Activation for Mullite Formation

Sample	$\triangle$ S* $(cal.deg.^{-1}mole^{-1})$
Na Halloysite	−49.0 to −51.3
Ca Halloysite	−30.4 to −31.9
Mn Halloysite	−21.6 to −25.3
Cu Halloysite	−6.0 to −9.4
Fe(III) Halloysite	−44.0 to −44.4
Untreated Halloysite	−0.44 to −6.45

If we assume that the transition state is unaffected by the

addition of impurities, then the ground state must be of a lower order for Fe(III), Ca, Mn and Na halloysites than for Cu or untreated halloysites, thus giving an increased rate of nucleation of mullite for the former samples.

All the known features of the reaction are explained by the following mechanism for the final stage of the reaction leading to mullite formation:

(a) Formation of mullite nuclei on the spinel particles by a rapid process obeying an exponential law.

(b) Rapid growth of crystals of mullite from these nuclei by a boundary controlled reaction, this being the rate determining step.

Migration of cations through the oxygen framework, occurs to give silicon rich and aluminium rich regions which ultimately yield cristobalite and mullite respectively. The rate of migration would be affected by cationic impurities, but the rate must be faster than that of the nucleation and growth of mullite, at least for short firing times.

REFERENCES — CHAPTER 5

(1) WAHL, F.M. and GRIM, R.E. in "Clays and Clay Technology",

(Ed. W.F. Bradley), 12th National Conference on Clays
and Clay Minerals (1963).

(2) PAULING, L.: "Nature of the Chemical Bond". 3rd Ed., Cornell
University Press, Ithica, New York (1960).

(3) LUNDIN, S.T.: "Studies on Triaxial Whiteware Bodies", p.107
(1959) Almquist and Wiksell, Stockholm.

(4) BUDNIKOV, P.P.: "Technologie der Keramik und der feuerfesten
Steine" (1953), Berlin.

(5) MACKENZIE, K.J.D.: "The Kinetics and Mechanism of the High
Temperature Solid State Reactions of Kaolinite Minerals".
M.Sc. Thesis, V.U.W. (1964).

(6) MCVAY, T.N.: J.Am.Ceram.Soc. 19, 195 (1936).

(7) TAYLOR, J.F.W.: Clay Min.Bull. 28, 53 (1962).

(8) JANDER, W.: Z. anorg. u. allgem. chem. 163, 1 (1927).

(9) BURKE, J.: Philosophical Magazine 5, 176 (1960).

(10) JACOBS, P.W.M.; and TOMPKINS, I.C.: "Chemistry of the
Solid State". Ed. Garner. p.184 (1955) Butterworth.